

Isonitriles as Stereoelectronic Chameleons: The Donor-Acceptor Dichotomy in Radical Additions

Gabriel dos Passos Gomes¹, Yulia Loginova,² Sergey Z. Vatsadze,² and Igor V. Alabugin*¹

¹: Department of Chemistry and Biochemistry, Florida State University, Tallahassee, USA. 32309 ;

²: Department of Organic Chemistry, Faculty of Chemistry, Lomonosov Moscow State University, 1-3 Leninskiye Gory, Moscow, Russia. 119991

*: corresponding author. alabugin@chem.fsu.edu

Abstract. Radical addition to isonitriles (isocyanides) starts and continues all the way to the TS mostly as a simple addition to a polarized π -bond. Only after the TS has been passed, the spin density moves to the α -carbon to form the imidoyl radical, the hallmark intermediate of the 1,1-addition-mediated cascades. Addition of alkyl, aryl, heteroatom-substituted and heteroatom-centered radicals reveals a number of electronic, supramolecular, and conformational effects potentially useful for the practical control of isonitrile-mediated radical cascade transformations.

Addition of alkyl radicals reveals two stereoelectronic preferences. First, the radical attack aligns the incipient $\text{C}\cdots\text{C}$ bond with the aromatic π -system. Second, one of the C-H/C-C bonds at the radical carbon eclipses the isonitrile N-C bond. Combination of these stereoelectronic preferences with entropic penalty explains why the least exergonic reaction (addition of the t-Bu radical) is also the fastest.

Heteroatomic radicals reveal further unusual trends. In particular, the Sn radical addition to the PhNC is much faster than addition of the other group IV radicals, despite forming the weakest bond. This combination of kinetic and thermodynamic properties is ideal for applications in control of radical reactivity via dynamic covalent chemistry and may be responsible for the historically broad utility of Sn-radicals (“the tyranny of tin”).

In addition to polarity and low steric hindrance, radical attack at the relatively strong π -bond of isonitriles is assisted by “chameleonic” supramolecular interactions of the radical center with both the isonitrile π^* -system and lone pair. These interactions are yet another manifestation of supramolecular control of radical chemistry.

Introduction

Isonitriles (isocyanides) combine rich and diverse reactivity^{1,2} with an intriguing dichotomy of electronic properties. Depending on the situation, one can think about an isonitrile as either a highly stabilized carbene or as a hetero-analogue of an alkyne. The latter description agrees very well with the nature of molecular orbitals and electron density distribution in the ground state isonitrile moiety. Isonitriles are isoelectronic to alkynes and resemble them in many ways. One can think of alkynes and isonitriles as “nuclear protomers” interconverted by a hypothetical process in which the atomic nucleus of the internal alkyne carbon “swallows” the terminal hydrogen to become a nitrogen atom. Although this unorthodox nuclear reaction changes the distribution of electron density, the nature of isonitrile molecular orbitals remains “alkyne-like” (with the exception of the alkyne sp-hybridized C-H bond becoming the isonitrile sp-hybridized lone pair). For example, both methyl acetylene and methyl isonitrile have two isoenergetic HOMOs and two isoenergetic LUMOs. Natural Bond Orbital (NBO) analysis of PhNC finds two π -orbitals with populations of 1.95-1.98 electrons (Figure 1).

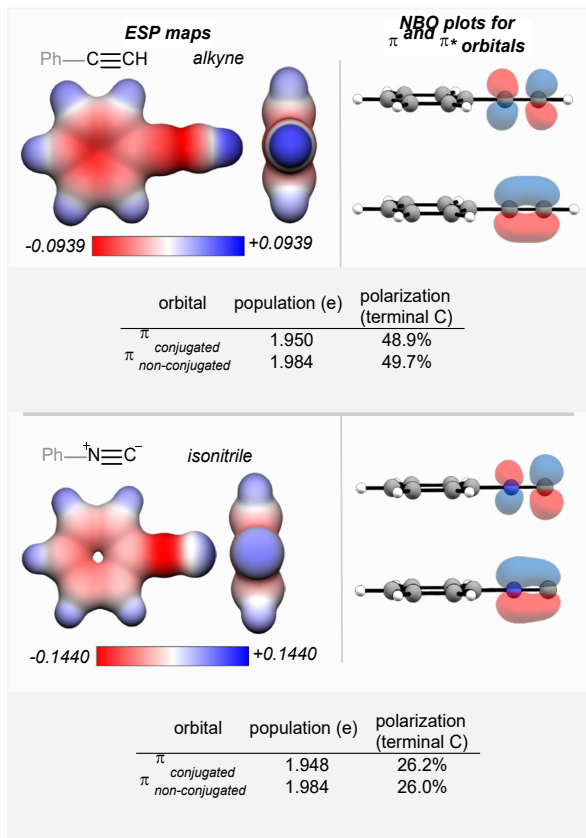
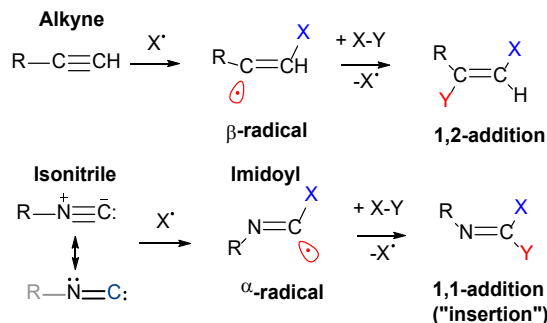


Figure 1. π -Bonds of isonitriles are similar to π -bonds of alkynes but more polarized – only 26% of electron density is at carbon.

Although electronically similar to alkynes, isonitriles display intriguing stereoelectronic features. For example, the ESP map reveals a sigma-hole at the C-end of the isonitrile. Sigma-holes have been shown to modulate stability and reactivity of supramolecular systems.³ Additionally, the isonitrile’s π^* -orbital is significantly more polarized than its alkyne counterpart due to the difference in electronegativity between carbon and nitrogen (Figure 1).

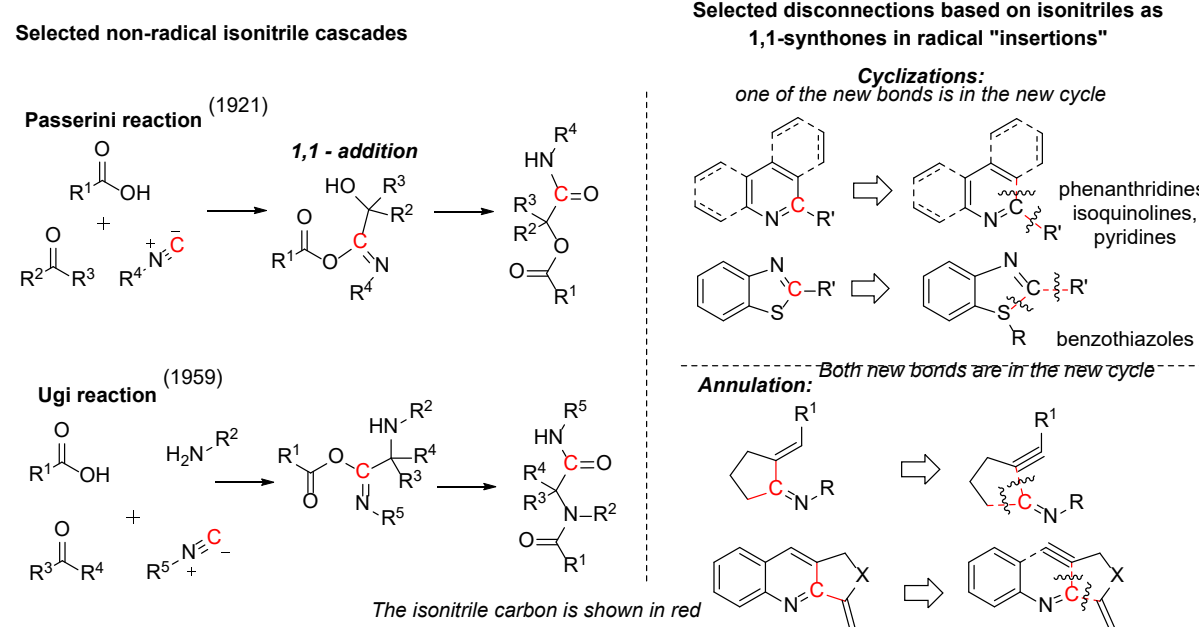
Importantly, the outcomes of additions to alkynes and isonitriles are drastically different. Whereas addition to alkynes proceeds in a “1,2-manner” where the new bonds are formed at the different alkyne carbons,

isonitriles can react as “1,1-synthons” by forming both new bonds at the same terminal carbon of the isonitrile moiety. Such outcome is consistent with the hidden carbene nature of the isonitrile functionality (Scheme 1).



Scheme 1. Isonitriles are isoelectronic to alkynes but display a "1,1"-addition pattern in radical reactions. If both X and Y were part of the same reagent X-Y, the 1,1-addition corresponds to the formal insertion of isonitrile carbon in an X-Y bond.

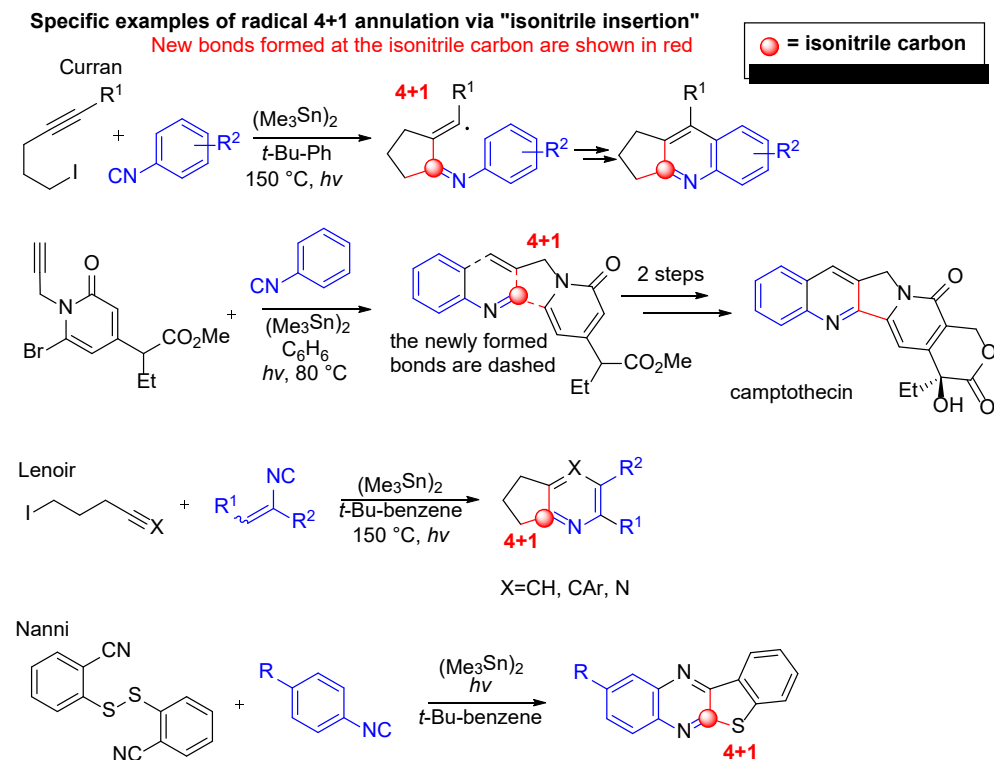
The ability of isonitriles to form two bonds at the same atom plays a key role in important multicomponent transformations such as the Passerini and the Ugi reactions (Scheme 2, left).^{1,4,5,6} Furthermore, the 1,1-bond formation pattern enabled in many interesting radical cascades of isonitriles, sometimes described as an “insertion of isonitrile” (Scheme 2, right).^{2b}



Scheme 2. Left. Isonitrile-based multicomponent reactions: Ugi and Passerini reactions. Right: Examples of radical annulations where isonitrile carbon serves as a corner of a new cycle.

The pioneering work of Curran and co-workers used isonitriles as radical acceptors in a number of imaginative radical cascade reactions where imidoyl radicals were used for construction of N-heterocycles (Scheme 3).⁷ For example, the [4+1] radical annulation strategy opened new paths towards medicinally important targets⁸ including the antitumor agent camptothecin.⁹ Subsequently, the [4+1] radical annulation of γ -iodoalkynes or iodonitriles were used to synthesize cyclopenta-fused pyridines and pyrazines.¹⁰ Nanni and co-workers successfully applied heteroatom-centered (sulfanyl) radicals for the synthesis of

cyclopentaquinoxalines.¹¹ Note that the size of the new cycle is defined by cyclization of the intermediate imidoyl radical (i.e., 5-exo for the [4+1] annulations). The potential 4-exo-cyclizations of radical formed from the 2nd annulation component in the first step of the cascade is slower than the intermolecular addition of this radical to the isonitrile. However, the addition step adds an extra carbon between the pendant functionality and the radical. At this point, the cyclization can proceed via a more favorable 5-exo path. This carefully designed competition of an intermolecular and two intramolecular radical reactions is remarkably elegant. However, kinetic requirements also impose certain limitations on the size of cycles accessible via this approach. Such limitations are overcome when the intramolecular radical trap is positioned at the isonitrile. The utility of the latter approach is illustrated by a number of biphenyl isonitrile cascades that lead to the formation of six-membered cycles, including substituted phenanthridines, isoquinolines, pyridines etc (Scheme 2, right).^{2, 12}



Scheme 3. Examples of radical annulations where the isonitrile carbon is “inserted” to connect two pre-installed functional groups of the 2nd reactant. The size of the new cycle is defined by cyclization of the intermediate imidoyl radical (i.e., 5-exo for the [4+1] annulations).

The above examples raise important questions about the “bipolar” nature of the isonitrile functionality. If isonitriles are polarized alkynes that can react as carbenes,¹³ when does the transition between these alkyne and carbene nature happen? Most importantly, do isonitriles retain the alkyne nature at the transition state (TS) or does the carbene nature take over before the TS is reached? This question is important for understanding and controlling isonitrile reactivity.

We will start by following the electronic changes during reaction of PhNC with the methyl radical in depth. Our goal will be to answer the intriguing question that we have asked earlier – when does the isonitrile moiety start to manifest its hidden carbene character, before or after the TS? This knowledge can guide rational design of radical additions to isonitriles.

Another goal of the present work is to evaluate the nature of radical-isonitrile interactions and compare orbital effects with sterics and electrostatics. To address these questions, we will expand computational

analysis to investigate, for the first time, reactivity of phenyl isonitrile towards a variety of radical sources at the same level of theory. The scope of this analysis includes a variety of alkyl and aryl radicals as well as several heteroatom-centered radicals. The broad variations in the nucleophilicity and electrophilicity of radicals will allow us to get insights into the chameleonic nature of isonitriles and the relative importance of electrostatic and orbital effects. We will also quantify the orbital interactions with NBO analysis.

Finally, after identifying the main trends for the activation barriers of these radical additions, we will compare them with the radical addition barriers of alkenes and alkynes with the goal of providing practical guidelines for the use of isonitriles in radical cascades.

Computational Details

Calculations were carried with the *Gaussian 09* software package,¹⁴ using the (U)M06-2X DFT functional¹⁵ (with an ultrafine integration grid of 99,590 points) with the 6-311++G(d,p) basis set for all atoms except of Sn and Ge, for which we have used the Def2-QZVPP¹⁶ basis set. Grimme's D3 version (zero damping) for empirical dispersion¹⁷ was also included. Frequency calculations were conducted for all structures to confirm them as either a minimum or a Transition State (TS). Intrinsic Reaction Coordinates (IRC)¹⁸ were determined for the TS of interest. Barriers were evaluated from isolated species due to formation of complexes for some systems, but not all of them. We performed Natural Bond Orbital¹⁹ (NBO) analysis on key intermediates and transition states. NBO deletions were performed at the UHF/6-311G(d) level of theory unless otherwise noted. Spin density was evaluated from the NBO analysis data. The Gibbs Free energy values are reported at 298 K, unless noted otherwise. We have used *GoodVibes*²⁰ by Funes-Ardoiz and Paton to obtain the temperature-corrected Gibbs Free energies for calculating the temperature effects on selectivity in multifunctional substrates.

We have also evaluated B3LYP²¹, B3LYP-D3 and ω B97X-D2²² functionals with the 6-311++G(d,p) basis set and ultrafine integration grid. Choice of methodology can be supported by internal consistency of thermodynamic data (for more details, see the ESI). The combination of the M06-2X with the D3 empirical dispersion correction was chosen for the evaluation of radical additions in order to provide an accurate estimate of supramolecular contributions to the transition state energies.

Results and discussion

Radical addition to isonitriles: “following electrons”, or how do isonitriles form two bonds at the same carbon in radical processes

As we discussed earlier, isonitriles and alkynes are isoelectronic. However, alkynes yield β -radicals in radical additions (i.e., the new radical center is formed at an atom *vicinal* to the point of radical attack) whereas isonitriles give α -radicals (i.e., the radical center is formed directly *at* the point of attack). Interestingly, analysis of geometries and electronic structures suggests that the radical addition transition states for alkynes and isonitriles are similar. In both cases, the addition proceeds as an attack at the triple bond following a Burgi-Dunitz trajectory.

In order to understand the details of these radical additions, we analyzed the spin density redistribution during the reaction. Initially, the spin density is concentrated at the reacting radical X (X=Me in Figure 2). As the radical gets closer to isonitrile, there is small but significant accumulation of radical character at nitrogen at the pre-TS distances of 2.4-2.2 Å. At these distances, the terminal carbon of the isonitrile (i.e., the α -atom), has less spin density than the nitrogen atom (i.e., the β -atom). This is exactly what one would expect from the classic radical addition to a π -bond. However, the α -carbon atom starts to gain progressively more of the radical character after the TS. At ~2 Å, the radical character at the α -carbon significantly exceeds the radical character at the β -nitrogen. At the even shorter C-X distances, the spin

density at the α -carbon continues to increase (up to 80%) whereas the spin density at the β -nitrogen remains nearly constant (at about 20%).

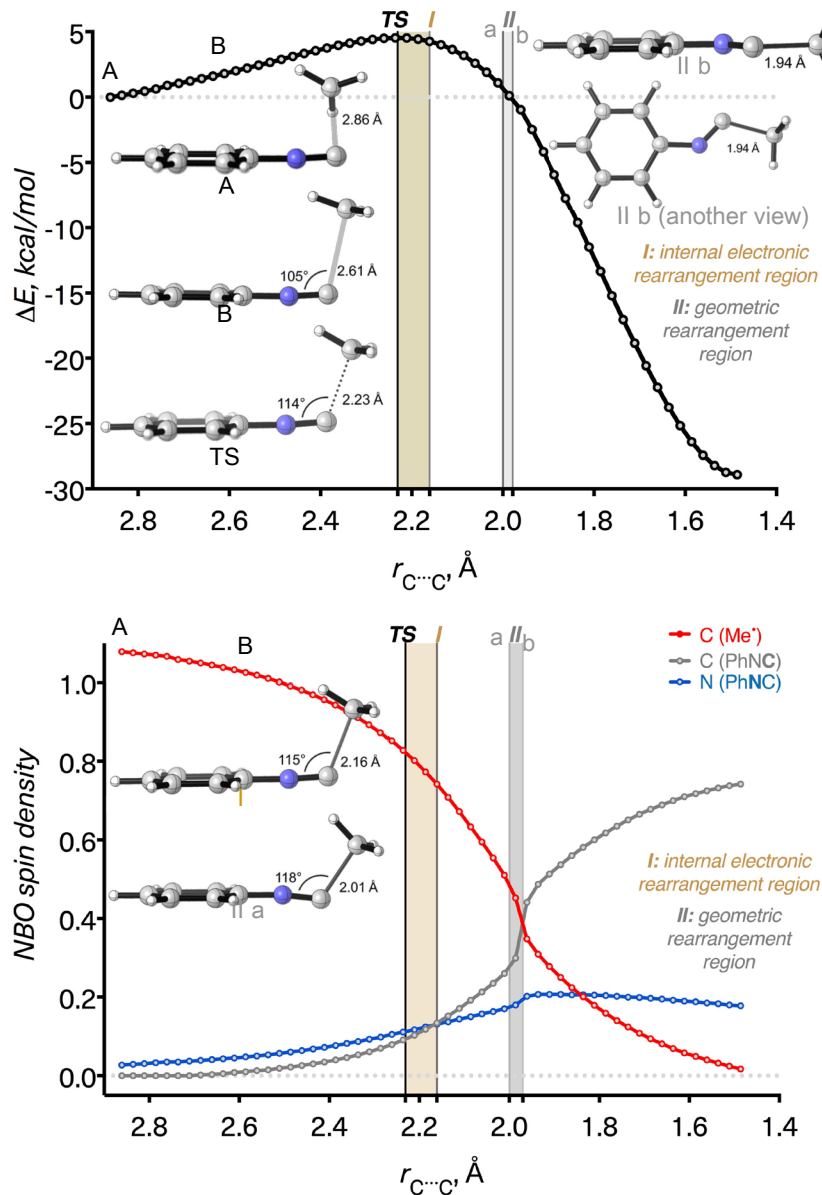
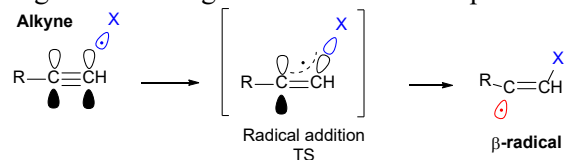


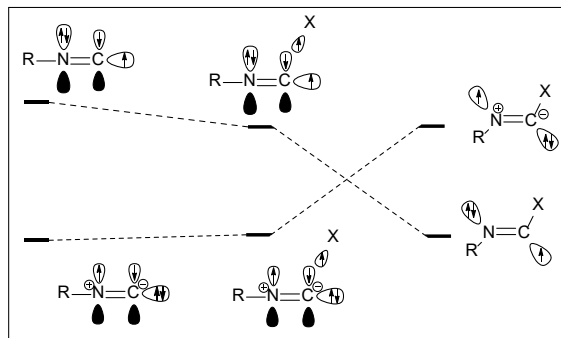
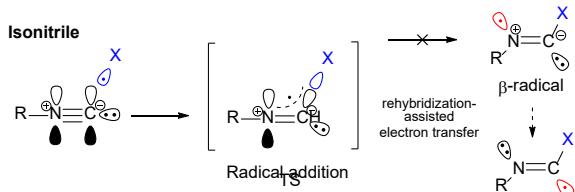
Figure 2. Potential energy profile (top) and evolution of spin density (bottom) for the addition of Me radical to PhNC

These data illustrate that radical addition to isonitriles indeed starts as an attack at the π -system and initially proceeds towards the N-centered β -radical. However, in parallel, the low energy sp-hybridized carbon-lone pair in isonitrile starts to rehybridize²³ to a higher energy $\sim\text{sp}^2$ lone pair as the C-X bond is being formed. At $\sim 2 \text{ \AA}$, the reaction progress leads to intramolecular charge transfer from the carbon lone pair to incipient radical orbital of the nitrogen, crossing to the electronic state that corresponds to the α -radical product (Scheme 4, bottom).

These changes account for the drastically different geometries for the TS and products of the radical additions to phenyl isonitrile. Out of the two orthogonal isonitrile π -orbitals, the attacking radical targets the one conjugated with the benzene π -system. After the TS, when the developing radical center at nitrogen is converted into a lone pair through the “rehybridization-assisted” electron transfer (Figure 2), the phenyl ring rotates to aligns itself with the acceptor $\text{N}=\text{C}$ π -bond instead of the nitrogen lone pair.

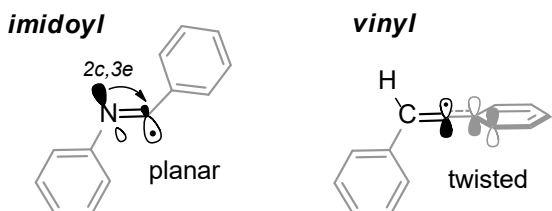


isonitriles are isoelectronic to alkynes but display a "1,1"-addition pattern:



Scheme 4. Comparison of radical additions to alkynes and isonitriles.

Although, the dominant Lewis structure in the imidoyl radical product is the one where the odd-electron density is at the α -carbon, the interaction between nitrogen lone pair and carbon radical remains strong and serves as a significant source of radical stabilization (i.e., the $2c,3e$ -bond).²⁴ Such interactions play an important role in structure and reactivity. For example, the Ph π -system is not conjugated with the radical center in the diphenyl imidoyl radical (in contrast to the case of the Ph-substituted vinyl radical). Since the radical center is already stabilized by the $3e$ -bond, the C-terminal of the Ph ring aligns instead with the out-of-plane π -system of the N=C moiety (Scheme 5). The perpendicular conformation is slightly higher in energy ($\Delta H = 0.3$ kcal/mol, $\Delta G = 0.6$ kcal/mol).

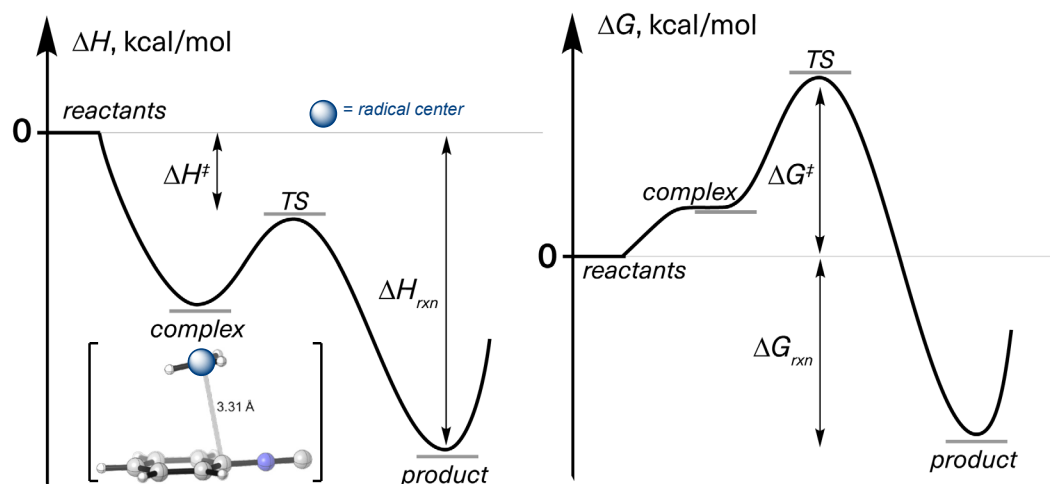


Scheme 5. Comparison of Ph-substituted vinyl and imidoyl radicals.

This picture agrees with the evaluation of natural charges throughout the reaction (the SI part). While the α -carbon of isonitrile remains mostly unchanged, nitrogen sees a slight decrease of its negative charge, with an interesting abrupt change in the opposite direction around region II in Figure 2. The most dramatic change is for the radical-bearing carbon of the attacking species. Its negative charge steadily increases through its addition to the isonitrile. The electrostatic pairing between the radical center and α -carbon of isonitrile is likely significant and contributes to reactivity.

Expanding the scope of radicals

Given the donor-acceptor dichotomy of isonitriles, we investigated the reactivity of phenyl isonitrile towards radicals of varying nature. A few technical comments need to be made before we proceed to the further discussion. The negative values for some of the calculated enthalpic barriers indicate the presence of pre-reaction complexes between the radical and the isonitrile. In several cases, we have calculated the structures of such complexes (examples of those are given in the SI). In all cases, the complexes are weak and strongly disfavored by the entropic factors (Scheme 6). In order to keep this discussion simple, we have chosen to report both the barriers and the reaction energies relative to the isolated reactants.



Scheme 6. Due to the formation of complexes activation barriers can lie below the energies of separated reactants. Left: Representative complex between Me-radical and PhNC shown. Right: At the Gibbs free energy PES, the formation of complexes often becomes an endergonic process due to entropic penalty of bringing two molecules together.

Alkyl radicals

Our starting point was the family of parent alkyl radicals with varying number of alkyl groups at the radical center. B3LYP calculations of Yoshida and coworkers estimated the free energy of activation for the addition of methyl radical to PhNC to be rather low (10.7 kcal/mol at 298 K).²⁵ Our (U)M06-2X(D3) calculations provided similar values (~13 kcal/mol at 298 K and ~16 kcal/mol at 363K). Furthermore, the enthalpic component of the barrier is only 5.7 kcal/mol, indicating that most of the free energy barrier comes from the unfavorable entropic contribution to the bimolecular process at elevated temperatures. The calculated free energy barrier is quite low. For example, it is lower than the barrier for the 7-10 kcal/mol more exergonic additions of methyl radical to phenyl acetylene and styrene (vide infra).

Table 1: Comparison of different DFT methods for the addition of Me-radical to PhNC (6-311++G(d,p) basis set)

Functional	ΔH^\ddagger	ΔH_{rxn}	ΔG^\ddagger	ΔG_{rxn}
UB3LYP	4.7	-24.2	12.0	-16.4
UB3LYP(D3)	3.0	-25.4	10.2	-16.9
U ω B97X(D2)	3.5	-27.4	12.7	-18.8
UM06-2X(D3)	5.1	-25.6	12.6	-15.7

We have expanded computational analysis to include larger alkyl radicals of different stability and steric bulk. The calculated energy profiles show the significant impact of substitution on the radical center. Counterintuitively, despite the increase in both stability and the steric bulk of the radical partners, the activation enthalpies continuously decrease from 5.1 to 0.6 kcal/mol upon the transition from the Me- to the *t*-Bu.

Table 2: Energies for addition of alkyl radicals to PhNC

R	ΔH^\ddagger	ΔH_{rxn}	ΔG^\ddagger	ΔG_{rxn}
Me	5.1	-25.6	12.6	-15.7
Et	3.4	-23.7	13.9	-12.0
<i>n</i> -Pr	3.2	-24.4	14.6	-12.1
<i>i</i> -Pr	2.4	-22.7	13.2	-10.4
<i>t</i> -Bu	0.6	-21.8	11.8	-9.0

The origin of this trend becomes apparent from a good correlation of the calculated activation enthalpies and nucleophilicity (estimated as *w*-values²⁸) of alkyl radicals. An equally good correlation is observed for the activation enthalpies vs. positive charge at the radical carbon (Figure 3).

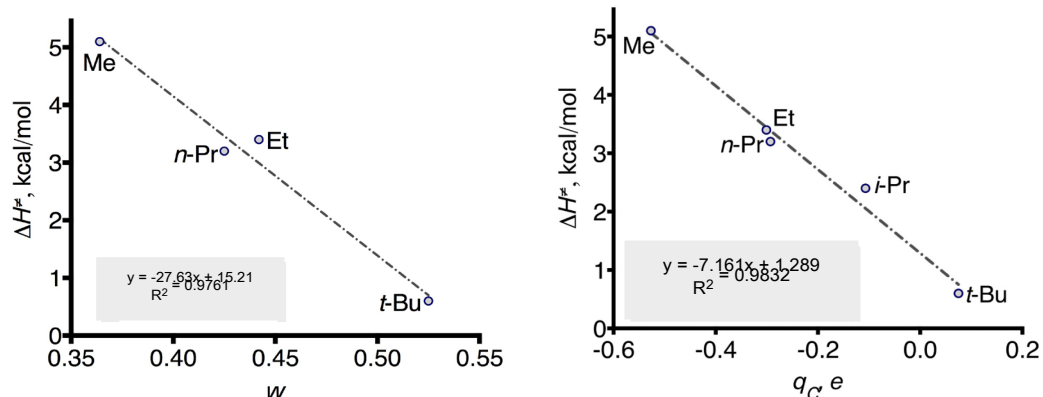


Figure 3. Activation enthalpy vs. nucleophilicity (left, nucleophilicity is estimated from the *w*-values²⁸) and vs. positive charge at the radical carbon (right) for Me, Et, *n*-Pr, *i*-Pr, and *t*-Bu radicals (the *w*-value for *i*-Pr radical is not available)

However, the trend for the free energy barriers ΔG^\ddagger is more complex (Figure 4). From Me to *n*-Pr, the ΔG^\ddagger values increase (Me<Et<*n*-Pr) but for more hindered *i*-Pr and *t*-Bu radicals the barriers *decrease*. Clearly, one cannot attribute this behavior to the increase in sterics at the more substituted radicals because the *bulkier* of the five studied alkyl radicals undergoes the *fastest* addition.

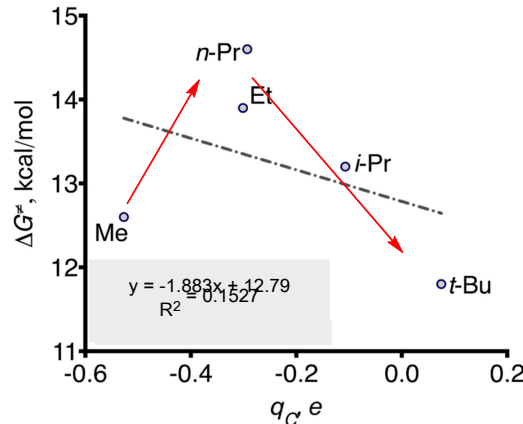
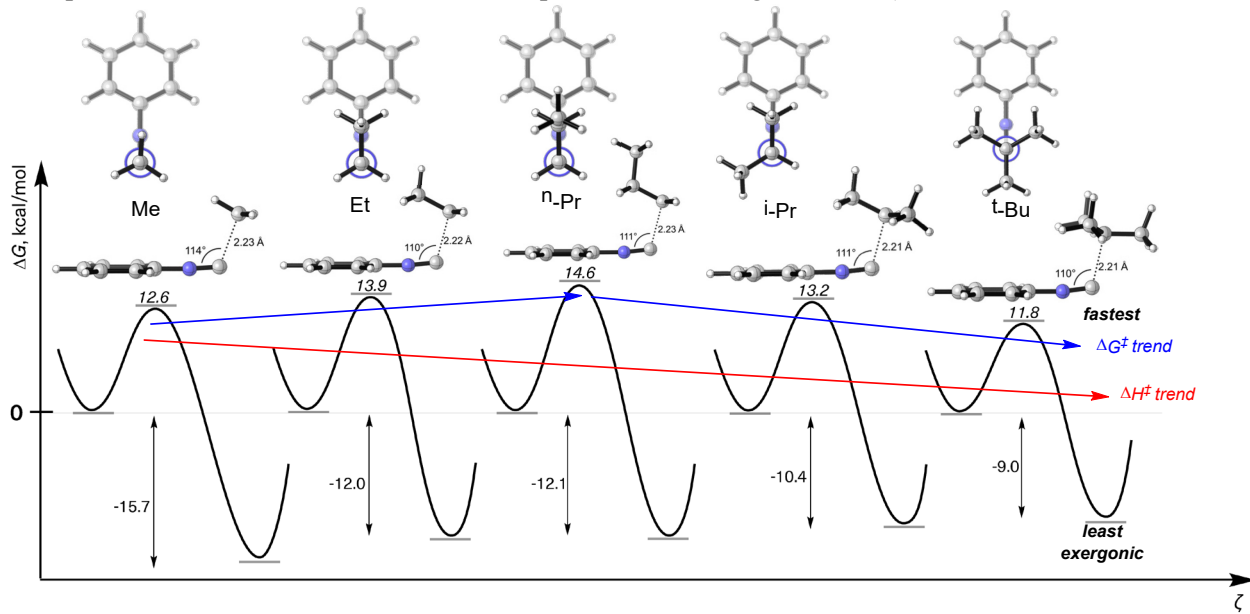


Figure 4. Correlation of the Gibbs activation barriers for alkyl radical additions to PhNC with the NBO charge at the radical carbon.

This interesting behavior stems from the tug-of-war between enthalpic and entropic factors. The nature of entropic effects becomes evident from the inspection of the TS geometries (Scheme 7).



Scheme 7. Potential energy surfaces and transition state structures for addition of alkyl-radicals to PhNC. Stereoelectronic preferences are illustrated by the Newman projections of the transition structures.

In every case, the radical attack at isonitrile reveals two stereoelectronic preferences. One is expected: the radical approach proceeds from a favorable²⁶ direction that aligns the incipient C...C bond with the aromatic π -system. The second structural preference is more subtle: in the transition states, one of the C-H/C-C bonds at the radical carbon prefers to eclipse the N-C bond of the attacked isonitrile (Scheme 7).²⁷ These geometries, along with the decreased NCC angles of attack, indicate the presence of an enthalpically

stabilizing through-space attractive interaction between the isonitrile and the alkyl groups. However, the preference for a specific conformation comes with the price of restricting the conformational freedom. Only the two symmetric radicals, i.e., methyl and *tert*-butyl, where all conformations are identical are free from this penalty.

The lower barrier found for the bulky *t*-Bu radical illustrates one of the other significant advantages of the isonitrile functionality as a radical acceptor. At the transition state stage, the carbon atom of the NC moiety offers little, if any, steric hindrance even to very bulky radical reagents. As the result, the *t*-Bu radical can fully manifest its higher nucleophilicity relative to that of the other alkyl radicals.²⁸ The steric effects start to come into play only once the C-C bond is fully formed in the product as illustrated by the steady decrease in reaction exergonicity with increased substitution at the radical: Me > Et > *n*-Pr > *i*-Pr > *t*-Bu. For this reason, the usual correlation between activation barriers and reaction exothermicity breaks down completely for this interesting family of reagents. *The least exergonic reaction (addition of the *t*-Bu radical) is also the fastest!*

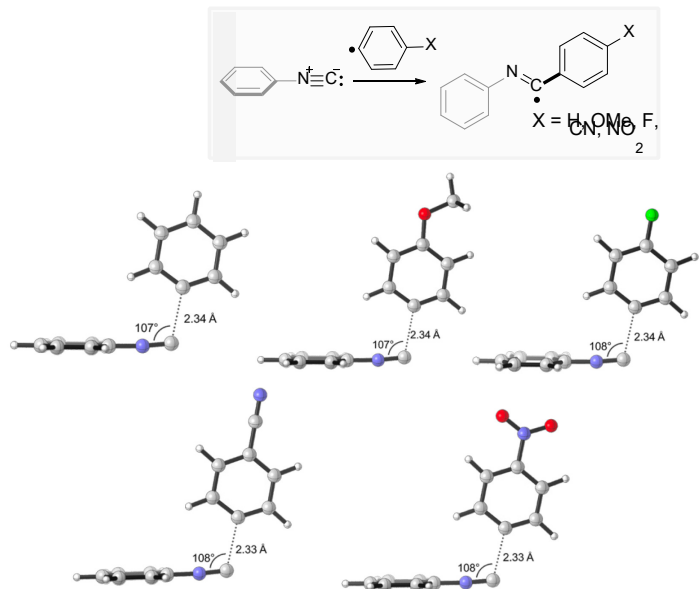
Para-substituted aryl radicals

In the next step, we have examined reactivity of PhNC towards aryl radicals (Scheme 8). All aryl radicals display much lower addition barriers in comparison to the alkyl radicals described in the previous section. The negative values for many of the calculated enthalpic barriers indicate the presence of pre-reaction complexes between the radical and the isonitrile (see the SI).

Interestingly, all *para*-substituents (both donors and acceptors) slightly lower the activation enthalpies and free energies for the addition of aryl-radicals in comparison to the addition of the parent Ph-radical. However, the variations are relatively small. The largest accelerating effect was observed for the nitro group, so the strongest acceptor does lead to the greatest barrier lowering, albeit only by 1.3 kcal/mol.

Table 3: Energies for addition of aryl radicals to PhNC

R	ΔH^\ddagger	ΔH_{rxn}	ΔG^\ddagger	ΔG_{rxn}
Ph	0.1	-38.7	9.6	-26.9
<i>p</i> -OMePh	-0.6	-40.8	9.3	-29.0
<i>p</i> -FPh	-0.3	-39.8	8.6	-28.4
<i>p</i> -CNPh	-0.8	-38.3	8.5	-26.6
<i>p</i> -NO ₂ Ph	-1.0	-38.3	8.3	-26.7
C ₆ F ₅	–	-40.9	4.8	-29.1

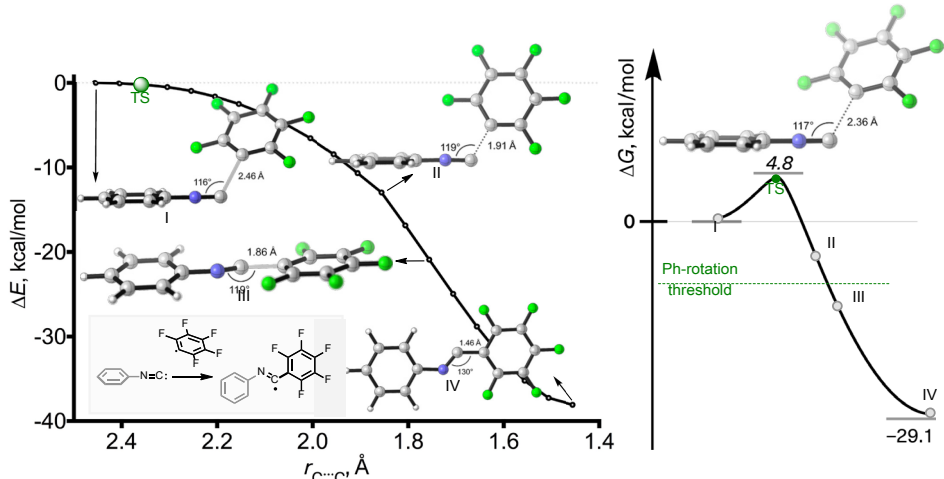


Scheme 8. Substituent effects on the energies and geometries for addition of *para*-substituted aryl radicals to PhNC.

As expected from the high reactivity and electrophilicity of aryl radicals, their transition states for the addition are quite early (C-C distance *ca.* 2.34 Å, Scheme 8). Interestingly, the earlier mentioned preference for the C-C bond of the radical to eclipse the CN bond of isonitrile is observed for the aromatic radicals as well. Note, that at these geometries, the interaction of the aromatic π -system with the isonitrile is inefficient, explaining why the substituents at the aromatic rings have a relatively small impact on the activation barriers. The additions follow the Bürgi-Dunitz trajectories with the NCC angle of $\sim 107^\circ$ (slightly smaller than the attack angle for the alkyl radicals). In the transition states, the two aromatic rings (of radical and isonitrile) are orthogonal to each other. The two aromatic π -systems align with the intervening C=N bond and with each other only later, in the addition product.

Remarkably, all barriers are predicted to be almost entirely entropic, originating from the penalty for bringing two reactants together in a bimolecular process. In all cases, except for the parent Ph group, the enthalpy of TS formation was negative, indicating the presence of attractive supramolecular interactions between the radical and isonitrile moieties that are greater in magnitude than the destabilizing distortion effects needed for the reactants to reach the transition state geometries.

To understand the effect of radical electrophilicity deeper, we have also explored the addition of perfluorophenyl radical to PhNC in more detail (Scheme 9). Whereas the *p*-F atom is an electron donor (electrophilic addition to the *p*-position of fluorobenzene is faster than addition to a single position of benzene²⁹), the *o*-F-substituent can also act as a powerful σ -acceptor.³⁰ A relaxed energy scan from the addition product was performed by stretching the newly formed C-C bond for 20 steps in 0.05 Å increments. This procedure allowed us to move backward along the IRC and locate the TS for the addition. This TS exists only on the free energy surface. Enthalpy of the C-C bond formation remains negative throughout the whole radical addition process. The observation that the most electrophilic of the aryl radicals is the most reactive (Scheme 8) *goes against* the trend discussed by us above for the alkyl radicals where lower barriers were found for more nucleophilic radicals (Figure 3).



Scheme 9. Addition of C_6F_5 -radical to PhNC has no enthalpic/electronic barrier

The reason why electrophilic aryl radicals show lower barriers than the nucleophilic alkyl radicals can be attributed to the higher exergonicity of aryl radical reactions. It is known that reaction exergonicity can provide a thermodynamic contribution to lowering the activation barriers. The extent of this barrier lowering can be evaluated from approximations that show how reaction barriers originate from the reactant and product potential energy surfaces.³¹ Application of this analysis suggests that, if the exergonicities were equal, each of the alkyl radical additions would be faster. In other words, although the addition of aryl radicals has a higher intrinsic barrier, this effect is masked by the ~11 kcal/mol increase in exergonicity

Heteroatom-centered and heteroatom-substituted radicals

Presence of additional α -heteroatoms at the radical carbon is known to significantly change electronic properties at the radical centers. To briefly probe such effects, we have calculated the reaction energy profiles for the hydroxymethyl and the trifluoromethyl radical addition to PhNC. Due to the presence of the lone pairs at oxygen, the hydroxymethyl radical is classified as strongly nucleophilic whereas CF_3 radical is considered highly electrophilic due to the combined inductive effect of the three fluorines.³²

Table 4: Energies for addition of heteroatom-centered and heteroatom-substituted radicals to PhNC

R	ΔH^\ddagger	ΔH_{rxn}	ΔG^\ddagger	ΔG_{rxn}
Et	3.4	-23.7	13.9	-12.0
HOCH₂	2.7	-18.8	12.7	-7.7
CF₃	0.0	-25.2	8.6	-13.5
MeNH	5.0	-30.0	15.8	-18.8
OMe	5.2	-24.9	15.0	-13.8
TEMPO		+9.0		+20.8

Reaction of the hydroxymethyl radical suffers from a ~ 4 kcal/mol thermodynamic penalty associated with the loss of a three-electron interaction between the radical center and the p-type lone pair of oxygen present in the reactant. However, despite this penalty, the Gibbs energy barrier addition is 1.2 kcal/mol lower than for the addition of ethyl radical (ethyl radical was taken as a reference point instead of methyl because of the entropic factors described in Scheme 7). This behavior is reminiscent of specific TS stabilization by three-electron through-bond interactions reported by us earlier.³³ It is also consistent with the lower TS energy for the radicals with increased nucleophilicity that we have discussed above for the alkyl groups.

From this point of view, it may seem surprising that the highly electrophilic CF_3 radical is even more reactive (4.0 kcal/mol free energy barrier lowering relative to the methyl radical) (Figure 5). Note that this behavior is similar to increased reactivity of C_6F_5 relative to C_6H_5 discussed earlier. This observation that radical addition is assisted by both the electron-donating and electron-accepting properties of the attacking radicals highlights the chameleonic behavior of isonitriles (Figure 5). One can also suggest that the pyramidalized CF_3 radical needs to undergo less distortion to reach the TS geometry.

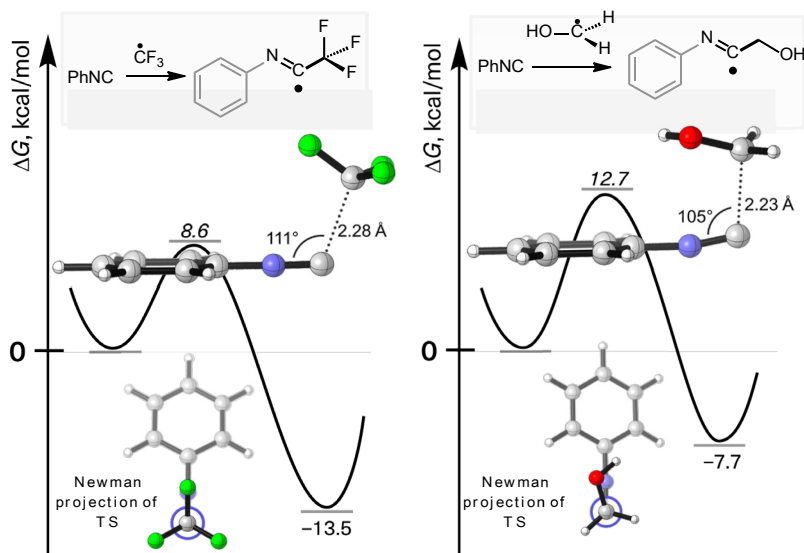
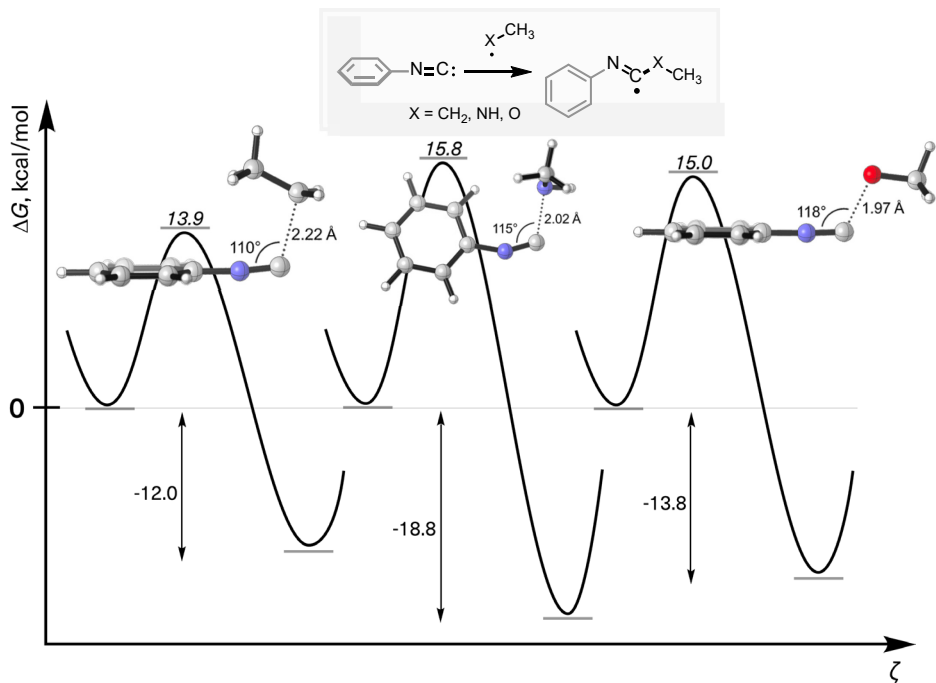


Figure 5. Geometries and energies for the addition of two heteroatom-substituted methyl radicals to phenyl isonitrile

On the other hand, the two heteroatom-*centered* radicals (OMe and NHMe) have higher barriers and their addition is less exergonic in comparison to the reaction of the ethyl radical. Interestingly, addition of the HNMe-radical proceeds via a TS where the attacked π -system is not in conjugation with the isonitrile phenyl group. This is the only case where we observe such behavior. This odd system has the highest barrier (15.8 kcal/mol) despite a relatively high exergonicity of -18.8 kcal/mol. We have also evaluated addition of the highly stabilized TEMPO radical and found it to be thermodynamically unfavorable ($\Delta G = +20.8$ kcal/mol).



Scheme 10. Geometries and energies for the addition of ethyl radical and two heteroatom-centered methyl radicals to phenyl isonitrile

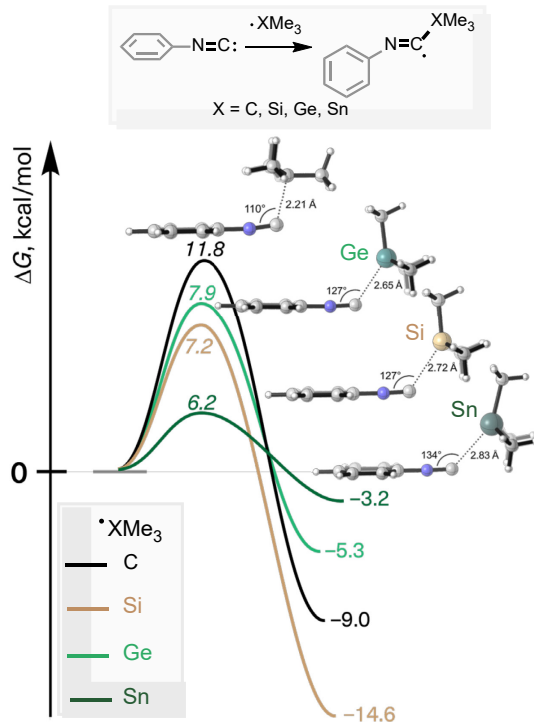
XMe₃ radicals – effect of orbital size

In the next step, we have also investigated the role of increasing atomic number in the radical additions using the heavier congeners of carbon: Si, Ge, and Sn. The barriers for the addition of these radicals are noticeably lower than for the addition of the t-Bu radical (6-8 kcal/mol vs. 12 kcal/mol, Table 5). An interesting feature in this progression is the unusual energetics for the reaction of trimethylsilyl (TMS) radical - it is the most exergonic of the four reactions but its activation barrier lies between Ge and Sn.

Table 5: Energies for addition of XMe₃ radicals to PhNC

R	ΔH^\ddagger	ΔH_{rxn}	ΔG^\ddagger	ΔG_{rxn}
Me ₃ C	0.6	-21.8	11.8	-9.0
Me ₃ Si	-1.4	-25.5	7.2	-14.6
Me ₃ Ge	-1.1	-15.9	7.9	-5.3
Me ₃ Sn	-2.7	-13.5	6.2	-3.2

Geometries of the four transition states are shown in Scheme 11. These geometries, again, illustrate the anomalous nature of the TMS radical addition – it has a much earlier addition TS than does the Ge radical. These computations also illustrate an interesting trend in the angle of attack – as the atom size increases, the trajectories become more and more obtuse (from 110° for t-Bu to 134° for Me₃Sn). For the heavier radicals, the radical orbital is not aimed at the isonitrile π^* orbital. One the other hand, the σ^*_{SnC} is positioned well for the overlap with the isonitrile lone pair.³⁴



Scheme 11. Transition State geometries for the group 14 XMe_3 ($\text{X} = \text{C, Si, Ge, Sn}$) radical additions. Note that Si/Ge transition does not follow the general trend (note that the C-C BDE is lower than the C-Si BDE in this system!).

Distortion-Interaction (DI) Analysis is a useful tool for analyzing bimolecular reactions.³⁵ We have applied it to understand the interplay between the destabilizing reactant distortions and attractive interactions between the reactants. In particular, we were interested whether the increase in the reactant pyramidalization (Scheme 11A) translates in the lower distortion energies for the radical additions.

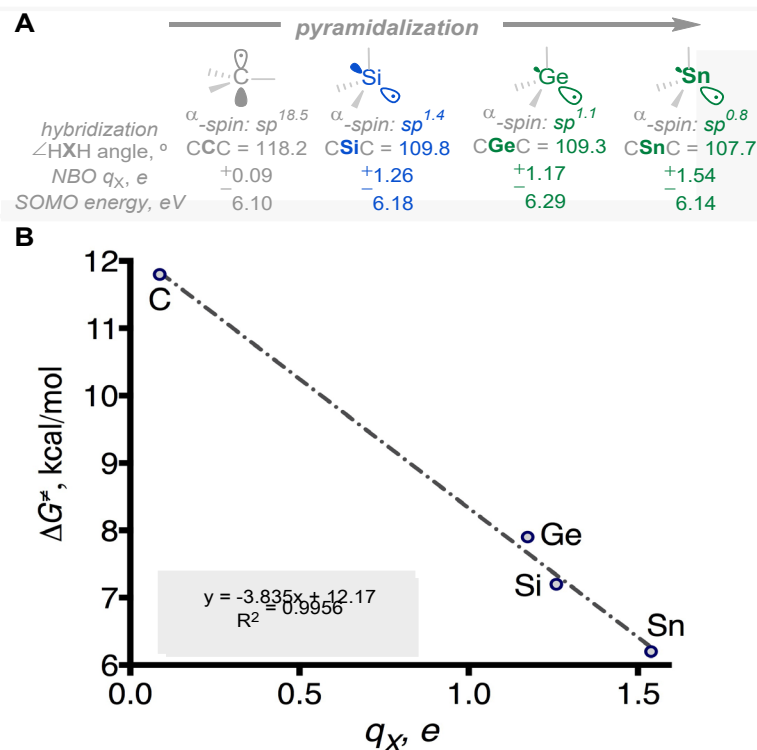
When activation energies are negative, the balance between distortion and interaction energies is dominated by the attractive interaction energies that serve as sources of TS stabilization. Not surprisingly, the distortion energy is very small even for the t-Bu radical (0.3 kcal/mol) and becomes even smaller for Si, Ge, and Sn (~0.1 kcal/mol). The interaction energies increase from C to Sn: C (1 kcal/mol) < Si ~ Ge (~2 kcal/mol) < Sn (~3 kcal/mol). Again, the Si-radical is “out of line” – its interaction energy is slightly more stabilizing than one would expect from a simple extrapolation from C to Ge.

Table 6: Distortion/interaction analysis for addition of XMe_3 radicals to PhNC (energies are in kcal/mol)

XMe_3	ΔE^\ddagger	$E_{dist}(\text{radical})$	$E_{dist}(\text{PhNC})$	$E_{dist}(\text{total})$	$E_{int}(\text{TS})$
C	-0.04	0.33	0.65	0.98	-1.03
Si	-1.8	0.06	0.10	0.16	-1.95
Ge	-1.4	0.07	0.16	0.23	-1.67
Sn	-3.1	0.11	0.03	0.14	-3.25

In order to get a deeper insight into the origin of these trends, we have determined additional electronic parameters for the four group IV radicals discussed in this section, i.e., hybridization of the radical centers

(evaluated by NBO analysis), natural charge at the radical atom, and energy of the Singly Occupied MO (the SOMO). Hybridization correlates with pyramidalization at the reaction center and with the distortion penalty for the radical attaining the TS geometry. The more pyramidalized radicals generally need to distort less to make a new bond. On the other hand, the more pyramidalized radicals also have more s-character in the radical orbital. Since the amount of s-character in non-bonding orbitals inversely correlate with their energy and donor properties, more pyramidalized radicals are expected to be less nucleophilic. Hence, the effect of radical hybridization on reactivity can be quite complex. An independent evaluation of the donor properties of the radicals, can be provided by the SOMO energy and by the atomic charges. The more electropositive, highly nucleophilic radicals are expected to have more positive charge at the central atom.



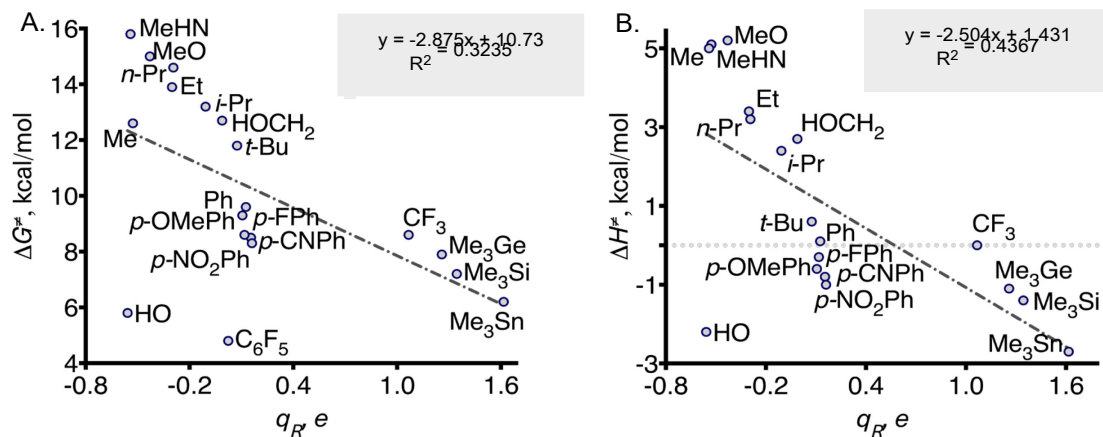
Scheme 12. A. Increase in pyramidalization of group 14 XMe_3 radicals. B: Correlation between natural charge at the radical-center for group IV elements and their free energy barriers towards addition to PhNC.

Interestingly, the best correlation between the individual electronic parameters and the calculated barriers was observed for the atomic charges at the radical center (Scheme 12). The greater positive charge at Si in comparison to Ge is consistent with the greater electronegativity of Ge.³⁶ In this correlation, the Si-radical addition is not anomalous.

The calculated data for the Sn-radical are noteworthy. It is the least exergonic of the four reactions in this section and it forms the weakest C-X bonds of the four group IV elements. However, it proceeds via the lowest barrier. This combination of properties accounts for the special advantage of the Bu_3Sn additions in organic radical chemistry (often referred to as “the tyranny of tin”³⁷). In particular, the reversibility of Sn-radical additions has been instrumental for the recent incorporation of this process in the arsenal of tools for dynamic covalent chemistry.³⁸

Global correlations: Interestingly, despite the excellent correlations observed for the selected groups of radicals, the global correlation between charge at the radical center and the calculated addition barriers is

weak. This weakness indicates the absence of a dominating factor and suggests that several effects, including sterics, electrostatics and orbital interactions, are likely contribute to the barrier heights.



Scheme 13. Global correlations for all radicals in this work. A. Correlation between natural charge at the radical-center for all evaluated systems and their activation free energies towards addition to PhNC. B: Same but for activation enthalpies.

An interesting observation from this complex behavior is that barriers for both the electrophilic and the nucleophilic radical addition to isonitriles can be quite low. In order to gain a deeper insight in the electronic effects in radical additions to isonitriles, we have evaluated orbital interactions using NBO analysis. Results of this analysis are discussed in the next section.

Supramolecular forces in the radical addition TS

In our analysis, we concentrated on the three odd-electron interactions shown in Figure 6. The interplay between these intermolecular interactions illustrates the chameleonic nature of isonitriles. This functional group combines a lone pair at carbon (a donor partner in supramolecular interactions) and a low energy π^* -CN orbital (an acceptor partner in supramolecular interactions). As the result, isonitriles can act as “stereoelectronic chameleons”,³⁰ serving as either a donor or an acceptor in supramolecular interactions depending on the nature of the interacting partner and its trajectory of approach for the isonitrile target. Because radical orbital is simultaneously half-full and half-empty, radicals can serve as a stereoelectronically flexible partner in such interactions. One can expect that depending on the electrophilic or nucleophilic nature of the radical, the preferred interaction pattern can adjust as the interacting species try to find the best compromise that takes advantage of the both donor and acceptor interactions.

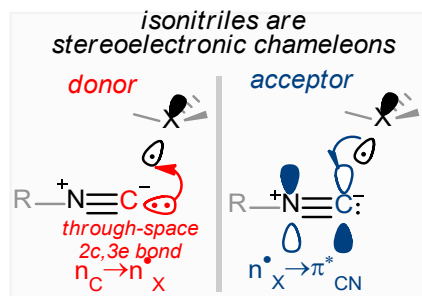
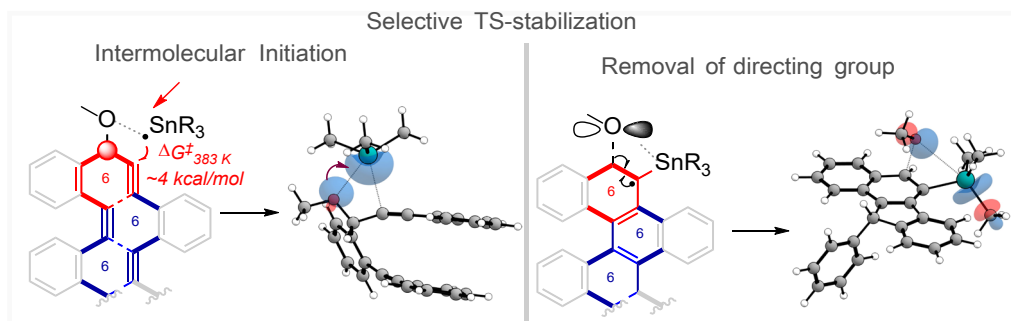


Figure 6. The ability of isonitriles to interact with both donor and acceptors accounts for their potential nature as stereoelectronic chameleons in radical additions.

Earlier, we have identified the directing role of through-space $2c,3e$ -interactions of radicals with a remote lone pair.³⁹ More specifically, such interaction between trialkyl tin radicals and one of the lone pairs at the α -OR substituent facilitates fast and selective addition of such radicals to propargylic ethers, enabling selective initiation of a cascade of exo-dig cyclizations.⁴⁰ An interesting feature of such cascades was their “boomerang” nature associated with the “return” of the radical center towards the directing OR group. As the radical arrives back at the α -carbon, it can assist in elimination of the directing group, rendering the latter “traceless”. Remarkably, this last step is also assisted by a through-space hyperconjugative interaction between the departing OR radical and the SnR_3 ’ group.⁴¹ The two new through-space interactions found in one cascade illustrate that supramolecular chemistry of radicals is likely to be more broad and diverse than it is presently recognized, thus urging for a systematic search of similar effects.



Scheme 14. Radical bonding in selective TS-stabilization for intermolecular initiation and removal of directing group.

The role of analogous through-space $2c,3e$ -interactions of radicals with a lone pair at a *C*-atom (Figure 6) has so far been unknown, even though such interactions can offer a new tool for supramolecular control in radical chemistry.

Similar to our earlier work,⁴² we employed NBO deletions to gauge the possible stabilizing impact for each of the interactions. In this approach, an off-diagonal element is deleted from the reduced one-electron density matrix in the NBO basis and the wavefunction energy is recalculated in single pass without variational reoptimization. The NBO deletions can be done for an individual interactions or for a group of them. Combined deletions can provide insights in cooperative or anti-cooperative relationship between different interactions.

A word of caution is needed before we proceed with the discussion. Although NBO analysis provides an opportunity to directly evaluate a balance of donor and acceptor interactions between two molecules, the accuracy of this method for the highly delocalized transition species is intrinsically lower than it is for the stable geometries where a dominant Lewis structure exists. For this reason, we will limit ourselves to comparison of only the relative magnitudes of the interactions. Their absolute values are expected to be very large since they describe breaking and making of chemical bonds far from energy minima. These large stabilizing interactions counteract the reactant distortion penalty and may ultimately evolve into formation of a new chemical bond. Their efficiency is illustrated by the negative activation enthalpies for several additions described earlier.

Because interaction energies depend on a variety of factors (such as distances, orientations and orbital energies for the partners) in a complex way, we will limit ourselves here to a general discussion and leave a more detailed analysis for a future work. In the present manuscript, our general goal is to provide the evidence for the importance of several types of donor-acceptor interactions where both the radical and the isonitrile can serve as either a donor or an acceptor. By comparing the two radical additions (Me and t-Bu) where the incipient bond distance is about the same, we will minimize the complications associated with the geometric effects on the orbital overlap.

Our specific goals will be to compare the donor and acceptor properties of radicals towards PhNC. Where does the balance lie in this chameleonic relationship? Are the radicals are predominantly acceptors towards PhNC or are they predominantly donors? Who is the acceptor and who is the donor? Of the two isonitrile donor orbitals, the π -bond and the lone pair, which one contributes more to the interaction with the half-filled radical orbital? And how do all these effects change for Me vs. t-Bu?

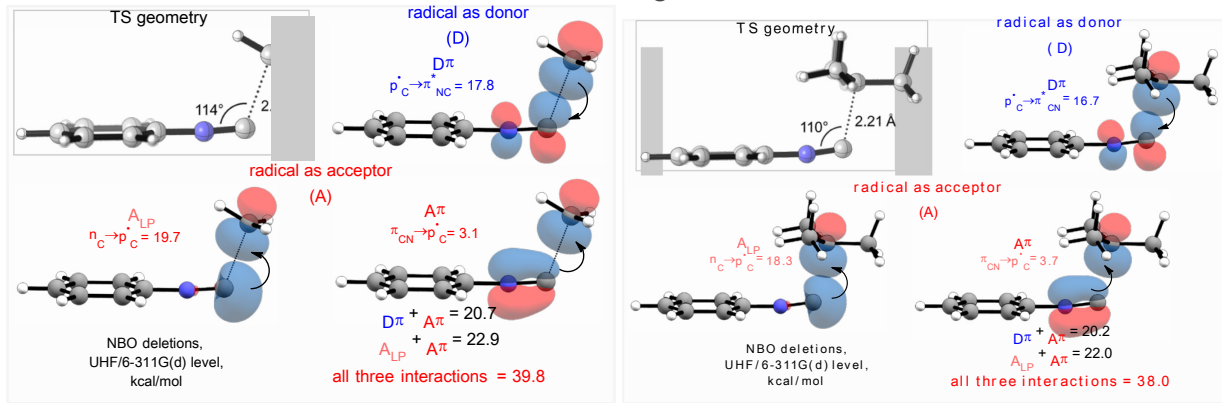


Figure 7. NBO interactions for the three odd-electron interactions identified in transition states for the addition of Me and t-Bu radicals to PhNC. The deletion energies are shown for each individual interaction and for selected combinations of the three interactions. D denotes interactions where the radical is a donor, A denotes interactions where the radical is an acceptor; subscript π refers to interaction with the isonitrile π or π^* orbital, subscript LP refers to interactions with the isonitrile lone pair.

The results of these studies are summarized in Figure 7 where we show deletion energies of each of the three individual interactions between isonitrile and the radical orbital (abbreviated as D_π , A_π , and A_{LP} in Figure 7) as well as the combined deletion energies for several interactions. The NBO relative energies are revealing and lead to a few conclusions summarized below.

The large differences in the relative magnitudes of radical interaction with the π and π^* isonitrile orbitals illustrates the electrophilic nature of the isonitrile π -system. The radicals act mostly as donors rather than acceptors in their interaction with the π system of PhNC, i.e., the D_π (17-18 kcal/mol) is much greater than A_π interaction (3-4 kcal/mol).

However, the lone pair of the isonitrile carbon changes the overall balance by serving as potent donor in the A_{LP} interaction with the radical that is even larger than the radical interaction with the isonitrile π^* (A_{LP} (18-20 kcal/mol) > D_π (17-18 kcal/mol)). When all three interactions are considered, the two interactions where radical serves as an acceptor ($A_\pi + A_{LP}$ (20-21 kcal/mol)) have greater energy than the single (D_π) interaction where the radical serves as a donor (17-18 kcal/mol). Comparison of the two interactions of radical with the π -bond ($D_\pi + A_\pi$) with the interaction with the lone pair A_{LP} illustrates that interactions with the π -bond are only slightly greater in magnitude than interaction with the lone pair (20-21 kcal/mol vs. 18-20 kcal/mol). *This duality of orbital donor/acceptor interactions indicates that isonitriles are stereoelectronically different from alkynes and alkenes in the radical addition reactions.* It is also obvious that radicals are chameleons as well – both donor and acceptor interactions between the radical center and the isonitrile moiety are very large. Remarkably, in reactions with isonitriles, even the “nucleophilic” radicals display acceptor properties! Of course, delocalization in this pair of interacting functionalities is “two-way”: the donor and acceptor interactions are balanced, and the overall charge transfer is small (see the following section).

As expected, interactions with the more stabilized t-Bu radical, on average are slightly smaller than the interactions with the much more reactive Me radical (38 vs. 40 kcal/mol for the combined interactions). Unexpectedly (based on the greater nucleophilicity of t-Bu radical), donation from the isonitrile p-orbital to the radical is slightly greater for the t-Bu radical (hence t-Bu radical is a slightly stronger acceptor than the Me radical towards the isonitrile p-orbital). However, the Me radical is slightly better acceptor towards the lone pair, i.e., the dominant isonitrile donor orbital (19.7 kcal/mol for Me vs. 18.3 kcal/mol for the t-Bu). Overall, there is no dramatic differences in the balance of the donor and combined acceptor orbital interactions for the two radicals. This finding suggests that electrostatic effects and, perhaps, dispersion⁴³ contribute to the lower barriers observed for the t-Bu radical addition.

This nature suggests that nucleophilic radicals should be excellent partners for isonitriles by taking advantage of the acceptor properties of the latter. However, the large “back donation” from the isonitrile lone pair to the radical orbitals offers stereoelectronic assistance to electrophilic radicals as well. From that point of view, isonitriles are, indeed, supramolecular chameleons, similar to carbenes in their ability to “adjust” to the reacting partner.

Electron transfer in the addition transition states:

The fundamental electronic feature of radicals is the unequal number of electrons with the opposite spins. To reflect this feature, NBO analysis treats the more numerous (α -) and less numerous (β -) spins separately. The overall description is a superposition of the two separate NBO structures. This treatment is well-suited for illustrating the chameleonic nature of radicals. In particular, the α -NBOs reflect the donor ability of a radical and the β -NBOs reflect the acceptor ability of a radical. Furthermore, in the relatively early TS for the radical additions, NBO analysis can readily separate the overall molecular system into the individual fragments and quantify the overall electron density (and its components) transferred between the fragments. In order to illustrate these features, let us analyze the total amount of electron density transferred to and from the radical to the target for the four radicals, Me, t-Bu, CF₃, and Me₃Sn (Table 7). For the methyl radical, we will also compare Ph acetylene and PhNC as the addition partners. As one can see, charge at the π -target (alkyne or isonitrile) is always negative for the α -spin and positive for the β -spin. Combining α - and β -spin charges describes amount and direction of the *overall* electron density transfer between the reagents. The combined density can be either negative (radical is the net donor) or positive (radical is the net acceptor).

Table 7: Charge transfer (in e) between selected radicals and their addition partners

PhC≡CH		PhNC		PhNC		
		Me		Me ₃ C	CF ₃	Me ₃ Sn
α	-0.113		-0.128	-0.158	-0.084	-0.095
β	+0.099		+0.122	+0.116	+0.102	+0.066
Σ	-0.014		-0.006	-0.042	+0.018	-0.029

Comparison of the methyl radical addition to Ph acetylene and Ph isonitrile reveals interesting differences. Both the α - (electron) and the β -spin (hole) densities at PhNC are greater than they are at Ph acetylene. This values illustrate that PhNC is both a better donor (-0.128 vs. -0.113 e) and the better acceptor (0.122 vs. 0.099 e) than its alkyne analog. In particular, the isonitrile is a better acceptor due to the greater polarization of the π^*_{NC} orbital and it is a better donor due to the presence of a lone pair at the isonitrile carbon, as described above. However, the *overall* electron density transfer from the radical is much smaller for addition to isonitrile relative to the alkyne (-0.006 vs. -0.014 e). The donor and acceptor abilities of PhNC and Me radical are balanced nearly perfectly. In this pair, the two interacting partners are both strong donors

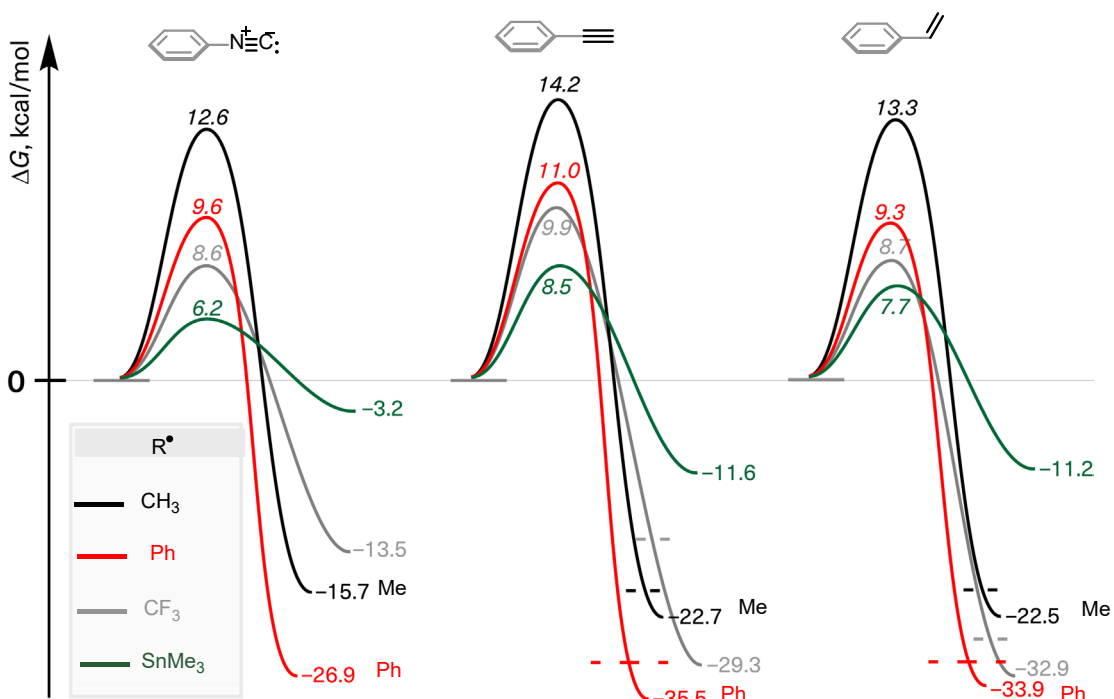
and strong acceptors but their donor/acceptor interactions in the “two-way” delocalization⁴⁴ or “donation / back-donation” (to borrow a term from the carbene chemistry) compensate each other almost perfectly. Comparison of these data with α -, β -, and total density transfers in the three more transition states (t-Bu, CF₃, and Me₃Sn addition to PhNC) suggest that the donor/acceptor synergy between radicals and isonitriles should be general but the balance depends on the partners. For example, the overall charge transfer for the CF₃ radical TS is positive (+0.018, i.e., the radical is an overall acceptor) whereas for the t-Bu and Me₃Sn radicals, these values are even more negative (-0.042 and -0.029 e) than for the Me radical.

The two directions of electron transfer in the addition TS can be described as contributions of two polar states in the curve-crossing model of radical reactivity.⁴⁵ This model was introduced by Shaik and Pross to describe the relation of activation barriers in terms of interactions of reactant and product electronic configurations (states). The model has been successfully applied to radical addition reactions by taking into account the interaction of four doublet states derived from the radical center and the target π -system. They include the ground state, the triplet state of the π -system, and the two possible charge-transfer states (R⁺A⁻ and R⁻A⁺, where A is the π -partner in the radical addition). In this model, the advantage of isonitriles in addition reactions with radicals is that additional polar states can contribute significantly to stabilization of the transition state by mixing to the overall wavefunction at the transition state geometry.

Selectivity of intermolecular radical addition: alkenes, alkynes, and isonitriles

In this section, we compare barriers and reaction energies for the radical additions to isonitriles, alkenes and alkynes using a selection of radicals of varying electro- and nucleophilicity: two nucleophilic (Me and Me₃Sn) and two electrophilic (Ph and CF₃), (Scheme 15). Three conclusions present themselves.

- 1) For each of the four radicals, additions to alkenes always have lower barriers than that additions to alkynes, despite having comparable or lower exergonicity. This is a consequence of the known fact that the alkyne π -bonds are generally stronger than the alkene π -bond⁴⁶ and is well supported by the available experimental data.⁴⁷
- 2) Although alkynes and isonitriles are isoelectronic, all four radical additions to isonitriles have lower barriers. This is remarkable because additions to isonitriles are *less* favorable thermodynamically than additions to alkynes (by 6-16 kcal/mol). This behavior suggests that intrinsic addition barrier³¹ to isonitriles are lower, likely due to the presence of additional TS stabilizing effects that are not present in alkynes.
- 3) The competition between alkenes and isonitriles is more complex: whereas the addition of nucleophilic radicals to isonitriles is faster than their addition to alkenes, the alkene addition barriers respond quicker to the increase in radical electrophilicity. As the result, the activation energies for addition of electrophilic radicals to alkenes and isonitriles are essentially identical. In other words, barriers for electrophilic radical additions to isonitriles do not increase, whereas barriers for nucleophilic radical additions are lowered in comparison to alkenes.



Scheme 15. Comparison of four radical additions to PhNC, Ph acetylene, and styrene

The free energy barrier for the nucleophilic radical (Me and SnMe_3) additions to PhNC is lower than the barrier for the >7 kcal/mol more exergonic additions of the same radical to phenyl acetylene and styrene

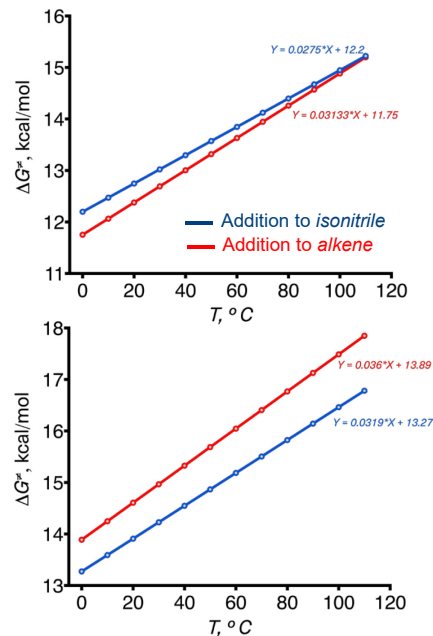
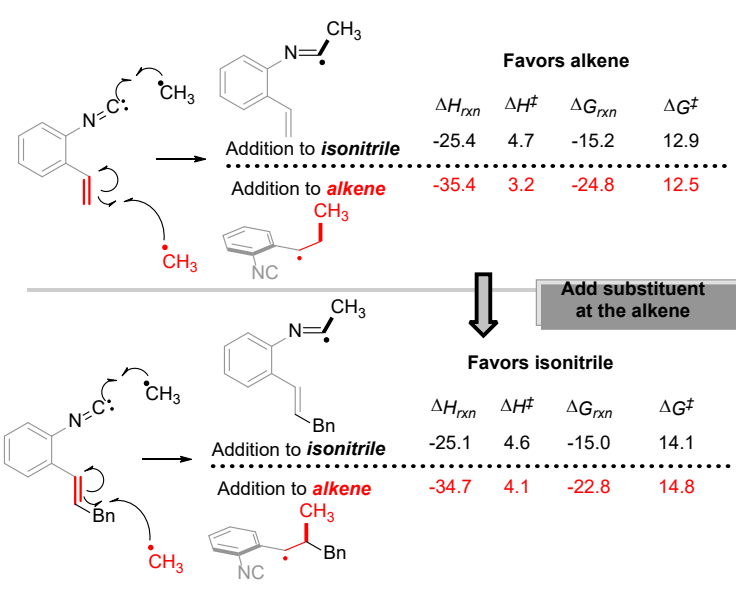
Chemoselectivity in addition to alkene-substituted- isonitriles:

Radical attack at isonitriles are often used for the initiation of radical cascades in the presence of other reactive functionalities. This selectivity is observed for the isonitrile group a variety of radical sources.² This method has gained attention during the past few years as a strategy to construct nitrogen containing heterocycles that are prevalent in biologically active molecules.²

A number of groups relied on selective addition at the isonitrile moiety of *o*-alkenylarylisonitriles using the $\text{HSnBu}_3/\text{AIBN}$ system.^{48,49} The reported yields vary strongly depending on the substitution. However, the origin of these effects remains unknown. In order to understand reactivity in these systems, we investigated barriers for radical additions to of alkenyl aryl isonitriles . We have also varied a nature of substitution at alkene to test how the greater steric hindrance at the alkenes may change the chemoselectivity.

Addition of the Me radical to the two functional groups of the *ortho* vinyl-substituted phenyl isonitrile shows the same trend as in the previous section. The free energy barriers are very close - addition to alkene is marginally faster (0.4 kcal/mol lower barrier at 298K). Larger entropic penalty for addition to alkene leads to temperature dependence that favors isonitriles at the higher temperatures.

Introduction of a benzyl group at the terminal alkene carbon has a large decelerating effect on the methyl radical addition to the alkene. Due to this change, the free energy barrier for the addition of Me radical to the substituted alkene group becomes higher than addition to the isonitrile. Free energy of activation for the addition to isonitrile change to a lesser extent. In fact, the free enthalpy does not change at all in comparison to *ortho*-vinyl substituted isonitrile and all of the slight increase in the Gibbs barrier comes from the entropic component.



Scheme 16. Left: Methyl radical additions to the isonitrile and alkene moieties in two alkenyl-substituted phenyl isonitriles at 298 K. Right: Temperature dependence of the activation free energy for these two additions

The main conclusion from results presented in this section is that selective addition to isonitriles in the presence of alkenes should not be taken for granted. From a practical point of view, these findings suggest two ways to control such selectivity. First, for selective addition to isonitriles in the presence of alkenes one should use sterically hindered nucleophilic radicals. Second, one can also take advantage of the more favorable entropy for additions to isonitriles by using higher temperatures. Isonitriles are less protected than alkenes by steric impediments at the carbon and the entropic penalty is paid only once whereas the two stabilizing orbital interactions that can occur at a range of attack geometries are synergistic and can reinforce each other.

Conclusions: Radical addition to isonitriles starts like a regular addition to a polarized π -bond and this similarity is preserved all the way to the transition state. Only after the TS is crossed, the developing N-radical takes advantage of rehybridization at the isonitrile carbon (a process that lifts the isonitrile lone pair energy) to transfer an electron from carbon. The relocation of the spin-center from nitrogen to carbon avoids charge separation and formation of a zwitter-ionic Lewis structure. The combination of addition to the π -orbital with the internal electron transfer leads to the hallmark 1,1-addition outcome that distinguishes isonitriles from their alkyne and alkene cousins and allows isonitriles to “insert” into bonds in radical processes. It also explains why, despite the conceptually different outcome, radical additions to isonitriles and alkynes have similar transition state structures.

However, the stereoelectronic analysis reveals that interesting hidden differences do exist between isonitriles and alkynes in their radical addition transition states. Isonitriles are chameleonic (like all carbenes and carbenoids³⁰) and are involved in a “back-bonding” interaction with the radical center that redirects electron density back to the radical. As the result, both electrophilic and nucleophilic radicals react with isonitriles readily.

Due to the intertwined combination of several electronic effects, the relationship between the radical nature and addition barriers is generally complicated. The frequent observation of a *less* exergonic addition being

faster indicates the presence of specific transition state stabilization effects, often different for different radical types.

The addition of alkyl radicals shows a strong dependence on the radical structure. In every case, the radical attack at isonitrile reveals two stereoelectronic preferences. One is expected: the radical approach proceeds from a favorable direction that aligns the incipient C••C bond with the aromatic π -system. The second structural preference is more subtle: in the transition states, one of the C-H/C-C bonds at the radical carbon prefers to eclipse the N-C bond of the attacked isonitrile. Interestingly, the sterically bulky but more nucleophilic radicals can react faster than their smaller analogs.

In particular, the lower barrier found for the bulky *t*-Bu radical illustrates one of the other significant advantages of the isonitrile functionality as a radical acceptor. At the transition state stage, the carbon atom of the NC moiety offers little sterical hindrance and allows the *t*-Bu radical to fully manifest its high nucleophilicity. The steric effects start to come into play only once the C-N bond is fully formed in the product as illustrated by the steady decrease in reaction exergonicity with increased substitution at the radical: Me > Et > *n*-Pr > *i*-Pr > *t*-Bu. For this reason, the usual correlation between activation barriers and reaction exothermicity breaks down - *the least exergonic reaction (addition of the *t*-Bu radical) is also the fastest!*

The greater reactivity of isonitriles (in comparison with alkenes and alkynes) towards hindered nucleophilic radicals can be attributed to π^*_{CN} polarization and the lack of steric hindrance for the attack at the isonitrile carbon. These selectivity trends should be useful in the design of radical cascades that include isonitriles in the presence of other reactive functionalities.

Para-substituents in aryl radicals show relatively weak effects at the addition barrier towards PhNC - the aryl π -system is not part of the reacting orbital array. Interestingly, both OMe and NO₂-substituted aryl radicals are more reactive than the Ph-radical itself. The C₆F₅ radical was found to be the most reactive of the investigated aryl radicals – the barrier for addition of this highly electrophilic species was found to be purely entropic. Heteroatomic substitution in the vicinity of radical center imposes a significant but complex influence.

The effect of orbital size in the family of C, Si, Ge, Sn-centered radicals is large. Although the observed barriers correlate best with electronegativity of the group IV atom, both Si and Sn display unique features. In particular, Me₃Si deviates from the expected correlations for barriers and reaction energies – the Me₃Si addition is highly exergonic and faster than the addition of the Me₃Ge radical. Me₃Sn is particularly interesting – despite making the weakest bond, the Sn radical addition to the PhNC is much faster than addition of the other group IV radicals. These features reinforce the special role of Sn-centered radicals in radical chemistry (i.e., the “tyranny of tin”) and their utility in radical dynamic covalent chemistry.

Finally, our results suggest practical lessons for the control of isonitrile reactivity in multifunctional substrates. Although alkynes and isonitriles are isoelectronic, the radical additions to isonitriles are less exergonic than additions to alkynes⁵⁰ but have lower barriers. The difference in kinetic and thermodynamic trends indicates that intrinsic addition barrier to isonitriles are lowered by the presence of additional TS stabilizing effects that are not present in alkynes. The present work identifies, for the first time, the contributions of stabilizing 2c,3e- interactions of radicals with a lone pair at the isonitrile carbon. Such interactions provide another illustration of the potential utility of supramolecular interactions between radicals and lone pairs for the control of radical chemistry.

The competition between alkenes and isonitriles is more complex and depends strongly on substitution. For the systems investigated herein, addition of nucleophilic radicals to isonitriles is faster than it is for alkenes whereas the barriers for addition of electrophilic radicals to alkenes and isonitriles are essentially identical. Selectivity can be shifted in favor of isonitrile by increasing steric bulk at the radical center and the alkene and by activating entropic preferences for addition to isonitriles at the high temperatures.

Supporting Information

Comparison of computational methods, additional details of NBO analysis, selected general trends for the radical additions to PhNC, as well as geometries and energies for all calculated structures reported in this work are available in the SI. This material is available free of charge via the Internet at <http://pubs.acs.org>

Acknowledgments

I.V.A and G. P. G. are grateful for the support of the National Science Foundation (Grant CHE-1800329). Computational resources were provided by NSF XSEDE (TG-CHE160006) and FSU Research Computing Center. S.Z.V and Y.D.L thank Russian Science Foundation (Grant # 16-13-00114).

References and Notes

¹ (a) Nenajdenko, V. G. *Isocyanide Chemistry*; Wiley-VCH Verlag & Co. KGaA: Weinheim, Germany, 2012. (b) Gulevich, A. V.; Zhdanko, A. G.; Orru, R. V. A; Nenajdenko, V. G. *Chem. Rev.* **2010**, *110*, 5235.

² (a) Zhang, B.; Studer, A. *Chem. Soc. Rev.*, **2015**, *44*, 3505. (b) Lei, J.; Huang, J.; Zhu, Q. *Org. Biomol. Chem.*, **2016**, *14*, 2593 (c) Chen, J. R.; Hu X. Q.; Lu, L. Q.; Xiao, W. J. *Chem. Rev.*, **2015**, *115*, 5301. (c) Giustiniano, M.; Basso, A.; Mercallli, V.; Massarotti, A.; Novellino, E.; Tron, G. C.; Zhu, J. *Chem. Soc. Rev.*, **2017**, *46*, 1295. (d) Qui, G.; Ding, Q.; Wu, J. *Chem. Soc. Rev.*, **2013**, *42*, 5257. (e) Song, B.; Xu, B. *Chem. Soc. Rev.*, **2017**, *46*, 1103. (f) Wille, U. *Chem. Rev.*, **2013**, *113*, 813.

³ Lim, J. Y. C; Beer, P. D. *Chem.* **2018**, *4*, 731.

⁴ Passerini, M.; Simone, L. *Gazz. Chim. Ital.*, **1922**, *52*, 126. Passerini, M.; Simone, L. *Gazz. Chim. Ital.*, **1922**, *52*, 181.

⁵ Ugi, I.; Meyr, R. *Angew. Chem.*, **1958**, *70*, 702. Ugi, I.; Meyr, R.; Steinbrückner, C. *Angew. Chem.*, **1959**, *71*, 386.

⁶ Bauer, F.; Braunschweig, H.; Schwab, K. *Organometallics* **2010**, *29*, 934.

⁷ Curran, D. P.; Liu, H. *J. Am. Chem. Soc.* **1991**, *113*, 6, 2127.

⁸ (a) Curran, D. P. Liu, H. *J. Am. Chem. Soc.*, **1992**, *114*, 5863. (b) Curran, D. P.; Sisko, J.; Yeske, P. E.; Liu, H. *Pure Appl. Chem.*, **1993**, *65*, 1153. (c) Curran, D.P.; Ko, S.-B.; Josien, H. *Angew. Chem. Int. Ed.*, **1996**, *34*, 2683. (d) Curran, D. P.; Liu, H.; Josien, H.; Ko, S.-B. *Tetrahedron*, **1996**, *52*, 11385. (e) Josien, H; Bom, D. *Chem. Lett.*, **1997**, *7*, 3189. (f) Frutos, O.D.; Curran, D.P. *J. Comb. Chem.*, **2000**, *2*, 639. (g) Spagnolo, P; Nanni, D; Encyclopedia of Radicals in Chemistry, Biology, and Materials, vol. 2, ed. C. Chatgilialoglu and A. Studer, Wiley, Chichester, **2012**, 1019.

⁹ Curran, D. P.; Ko, S.-B.; Josien, H. *Angew. Chem., Int. Ed. Engl.* **1995**, *34*, 2683.

¹⁰ Lenoir, I.; Smith, M. L. *J. Chem. Soc., Perkin Trans. 1* **2000**, 641.

¹¹ Camaggi, C. M.; Leardini, R.; Nanni, D.; Zanardi, G. *Tetrahedron* **1998**, *54*, 5587.

¹² Selected examples: (a) Shaw, D. H.; Pritchard, H. O. *Can. J. Chem.* **1967**, *45*, 2749. (b) Rigby, J. H.; Qabar, M.; Ahmed, G.; Hughes, R. C. *Tetrahedron* **1993**, *49*, 10219. (c) Tobisu, M.; Koh, K.; Furukawa, T.; Chatani, N. *Angew. Chem., Int. Ed.*, **2012**, *51*, 11363. (d) Wang, Q.; Dong, X.; Xiao, T.; Zhou, L. *Org. Lett.*, **2013**, *15*, 4846. (e) Li, Z.; Fan, F.; Yang, J.; Liu, Z.-Q. *Org. Lett.*, **2014**, *16*, 3396. (f) Pan, C.; Han, J.; Zhang, H.; Zhu, C. *J. Org. Chem.*, **2014**, *79*, 5374. (g) He, Z.; M. Bae, J. Wu, T. F. Jamison, *Angew. Chem., Int. Ed.*, **2014**, *53*, 14451. (h) Zhang, B.; Studer, A. *Org. Biomol. Chem.*, **2014**, *12*, 9895. (i) Tokuyama, H.; Watanabe, M.; Hayashi, Y.; Kurokawa, T.; Peng, G.; Fukuyama, T. *Synlett*, **2001**, 1403. (j) Zhang, B.; Studer, A. *Org. Lett.*, **2014**, *16*, 1216. (k) Bujok, R.; Cmoch, P.; Wrobel, Z. *Tetrahedron Lett.* **2014**, *55*, 3410. (l) Tong, K.; Zheng, T.; Zhang, Y.; Yu, S. *Adv. Synth. Catal.*, **2015**, *357*, 3681. (m) Wang, Q.; Dong, X.; Xiao, T.; Zhou, L. *Org. Lett.*, **2013**, *15*, 4846. (n) Mitamura, T.; Iwata, K.; Ogawa, A. *Org. Lett.*, **2009**, *11*, 3422. (o) Xia, Z.; Huang, J.; He, Y.; Zhao, J.; Lei, J.; Zhu, Q. *Org. Lett.*, **2014**, *16*, 2546. (p) Janza, B.; Studer, A. *Org. Lett.*, **2006**, *8*, 1875. (r) Tobisu, M.; Fujihara, H.; Koh, K.; Chatani, N. *J. Org. Chem.*, **2010**, *75*, 4841.

¹³ For other examples of carbene reactivity of alkynes see: (a) Alabugin, I. V.; Gold, B. *J. Org. Chem.*, **2013**, *78*, 7777. (b) Zeidan, T.; Kovalenko, S. V.; Manoharan, M.; Clark, R. J.; Ghiviriga, I.; Alabugin I. V. *J. Am. Chem. Soc.* **2005**, *127*, 4270.

¹⁴ Frisch, M. J. *et al.* Gaussian 09, Revision D.01; Gaussian: Wallingford, CT, 2009. Complete reference in the SI.

¹⁵ (a) Zhao, Y.; Truhlar, D. G. *Theor. Chem. Acc.*, **2008**, *120*, 215. (b) Zhao, Y.; Truhlar, D. G. *Acc. Chem. Res.*, **2008**, *41*, 157.

¹⁶ The Def2-QZVP basis set for Sn was obtained at Basis Set Exchange (<https://bse.pnl.gov/bse/portal>): (a) Feller, D. *J. Comp. Chem.*, **1996**, *17*, 1571; (b) Schuchardt, K. L.; Didier, B. T.; Elsethagen, T.; Sun, L.; Gurumoorthi, V.; Chase, J.; Li, J.; Windus, T. L. *J. Chem. Inf. Model.*, **2007**, *47*, 1045. (c) reference for the basis set: Weigend, F.; Ahlrichs, R.; *Phys. Chem. Chem. Phys.*, **2005**, *7*, 3297.

¹⁷ Grimme, S.; Antony, J.; Ehrlich, S.; Krieg, H. *J. Chem. Phys.*, **2010**, *132*, 154104.

¹⁸ Fukui, K. *Acc. Chem. Res.*, **1982**, *14*, 363.

¹⁹ (a) Weinhold, F.; Landis, C. R.; Glendening, E. D. *International Reviews in Physical Chemistry* **2016**, *35*, 1. Reed, A. E.; Weinhold, F. *J. Chem. Phys.*, **1985**, *83*, 1736. (b) Reed, A. E.; Weinhold, F. *Isr. J. Chem.*, **1991**, *31*, 277. (c) Reed, A. E.; Curtiss, L. A.; Weinhold, F. *Chem. Rev.*, **1988**, *88*, 899. (d) Weinhold F. in Schleyer P.v.R. *Encyclopedia of Computational Chemistry*: Wiley: New-York, **1998**, *3*, 1792. Selected recent applications of NBO analysis towards analysis of organic structure and reactivity: a) Podlech, J. *J. Phys. Chem. A* **2010**, *114*, 8480. b) Freitas, M. P. *J. Org. Chem.* **2012**, *77*, 7607. c) Greenway, K. T.; Bischoff, A. G.; Pinto, B. M. *J. Org. Chem.* **2012**, *77*, 9221. d) Juaristi, E.; Notario, R. *J. Org. Chem.* **2015**, *80*, 2879. e) Gomes, G. P.; Vil', V.; Terent'ev, A.; Alabugin, I. V. *Chem. Sci.* **2015**, *6*, 6783. f) Vidhani, D.; Krafft, M.; Alabugin, I. V. *J. Am. Chem. Soc.*, **2016**, *138*, 2769. g) V. A. Vil', G. dos Passos Gomes, O. V. Bityukov, K. A. Lyssenko, G. I. Nikishin, I. V. Alabugin, A. O. Terent'ev, *Angew. Chem. Int. Ed.*, **2018**, *57*, 3372.

²⁰ Funes-Ardoiz, I.; Paton, R. S. *GoodVibes*, v2.0.1; **2017**, doi:10.5281/zenodo.884527

²¹ (a) Becke, A. D. *J. Chem. Phys.*, **1993**, *98*, 5648. (b) Lee, C.; Yang, W.; Parr, R. G. *Phys. Rev.*, **1988**, *B 37*, 785

²² Chai, J.-D.; Head-Gordon, M. *Phys. Chem. Chem. Phys.* **2008**, *10*, 6615.

²³ Alabugin, I. V.; Bresch S.; Gomes, G. P. *J. Phys. Org. Chem.*, **2015**, *28*, 147-162

²⁴ The bent geometry at both the N and the C centers of the imidoyl radical is associated with the penalty for rehybridization. Although the linear geometry would maximize the stabilizing effect of 3e-interaction between the lone pair and the radical, achieving this geometry would compromise preferred hybridization states of the two centers. For a more general discussion of rehybridization effects, see ref. 23. For a more specific discussion of electronic effects at nitrogen, see: Alabugin I. V.; Manoharan, M.; Buck, M.; Clark, R. *THEOCHEM*, **2007**, *813*, 21. Alabugin, I. V.; Bresch S.; Manoharan, M. *J. Phys. Chem. A* **2014**, *118*, 3663. Borden, W. T. *J. Phys. Chem. A*, **2017**, *121*, 1140.

²⁵ Yamago, S.; Miyazoe, H.; Goto, R.; Hashidume, M.; Sawazaki, T.; Yoshida, J. *J. Am. Chem. Soc.* **2001**, *123*, 3697.

²⁶ Alabugin, I. V. *Stereoelectronic Effects: the Bridge between Structure and Reactivity*. John Wiley & Sons Ltd, Chichester, UK, 2016.

²⁷ The only case where this geometric preference is not observed is the *t*-Bu addition TS.

²⁸ Vleeschouwer, F.; Speybroeck, V.; Waroquier, M.; Geerlings, P.; Proft, F. *Org. Lett.*, **2007**, *9*, 2721.

²⁹ Rosenthal, J.; Schuster, D. *J. Chem. Educ.* **2003**, *80*, 679

³⁰ Vatsadze, S. Z.; Loginova, Y. D.; Gomes, G.; Alabugin, I. V. *Chem. Eur. J.*, **2017**, *23*, 3225.

³¹ In short, about one-half of reaction exergonicity is translated into barrier lowering. For a more accurate evaluation of thermodynamic effects on the intrinsic activation barrier in radical reactions via Marcus theory, see: Alabugin I.V.; Manoharan, M. *J. Am. Chem. Soc.* **2005**, *127*, 12583. Alabugin I.V.; Manoharan, M. *J. Am. Chem. Soc.* **2005**, *127*, 9534.

³² Heberger, K.; Lopata, A. *J. Org. Chem.*, **1998**, *63*, 8646.

³³ Mondal, S.; Gold, B.; Mohamed, R. K.; Alabugin, I. V. *Chem. Eur. J.*, **2014**, *20*, 8664. Mohamed, R.; Mondal, S.; Gold, B.; Evoniuk, C. J.; Banerjee, T.; Hanson, K.; Alabugin, I. V. *J. Am. Chem. Soc.*, **2015**, *137*, 6335.

³⁴ Harris, T.; Gomes, G. P.; Ayad, S.; Clark, R. J.; Lobodin, V. V.; Tuscan, M.; Hanson, K.; Alabugin, I. V. *Chem.*, **2017**, *3* (4), 629.

³⁵ (a) Bickelhaupt, F. M.; Houk, K. N. *Angew. Chem. Int. Ed.* **2017**, *56*, 10070. (b) Ess, D. H.; Houk, K. N. *J. Am. Chem. Soc.* **2007**, *129*, 10646. (c) Utility in catalyst design: Gomes, G. P.; Alabugin, I. V. *J. Am. Chem. Soc.*, **2017**, *139*, 3406.

³⁶ Allred, A.L.; Rochow, E.G. *J. Inorg. And Nucl. Chem.*, **1958**, *5*, 269.

³⁷ Baguley, P. A.; Walton, J. C.; *Angew. Chem., Int. Ed. Engl.*, **1998**, *37*, 3072.

³⁸ Mondal, S.; Mohamed, R. K.; Manoharan, M.; Phan, H.; Alabugin, I. V. *Org. Lett.*, **2013**, *15*, 5650.

³⁹ (a) Pati, K.; Gomes, G. P.; Harris, T.; Hughes, A.; Phan, H.; Banerjee, T.; Hanson, K.; Alabugin, I. V. *J. Am. Chem. Soc.* **2015**, *137*, 1165. (b) Pati, K.; Gomes, G. P.; Alabugin, I. V. *Angew. Chem. Int. Ed.* **2016**, *55*, 11633.

⁴⁰ For the utility of exo-dig cascades, see: I. V. Alabugin, E. Gonzalez-Rodriguez. *Acc. Chem. Res.*, **2018**, *51*, 1206. Gilmore, K.; Mohamed, R. K.; Alabugin, I. V. *WIREs: Comput. Mol. Sci.* **2016**, *6*, 487.

⁴¹ Harris, T.; Gomes, G.; Clark, R. J.; Alabugin, I. V. *J. Org. Chem.*, **2016**, *81*, 6007.

⁴² For example: Gold, B.; Dudley, G. B.; Alabugin, I. V. *J. Amer. Chem. Soc.*, **2013**, *135*, 1558. Vidhani, D.; Krafft, M.; Alabugin, I. V. *J. Am. Chem. Soc.*, **2016**, *138*, 2769.

⁴³ Wagner, J. P.; Schreiner, P. R. *Angew. Chem., Int. Ed.* **2015**, *54*, 12274.

⁴⁴ Alabugin, I. V.; Gomes, G.; Abdo, M. A. *WIREs: Comput. Mol. Sci.* **2018**;e1389, <https://doi.org/10.1002/wcms.1389>.

⁴⁵ Pross, A. *Adv. Phys. Org. Chem.* **1985**, *21*, 99–196. Shaik, S. S. *Prog. Phys. Org. Chem.* **1985**, *15*, 197–337.

⁴⁶ Nicolaides, A.; Borden, W. T. *J. Am. Chem. Soc.* **1991**, *113*, 6750. The same conclusion arises from the application of the Shaik-Pross curve-crossing model as a consequence of the greater singlet-triplet gap: Gómez-Balderas, R.; Coote, M. L.; Henry, D. J.; Fischer, H.; Radom, L. *J. Phys. Chem. A* **2003**, *107*, 6082. See also: Fischer, H.; Radom, L. *Angew. Chem., Int. Ed.* **2001**, *40*, 1340.

⁴⁷ Holt, P. M.; Kerr, J. A. *Int. J. Chem. Kinet.* **1977**, *9*, 185–200. Giese, B.; Lachhein, S. *Angew. Chem., Int. Ed. Engl.* **1982**, *21*, 768. Nam, G; Tokmakov, I.V.; Park, J.; Lin, M. C. *Proc. Combust. Inst.*, **2007**, *31*, 249.

⁴⁸ 5-Exo-radical-cyclizations of *o*-alkenyl arylisocyanides with organotin reagents: (a) Kobayashi, S.; Peng, G.; Fukuyama, T. *Tetrahedron Lett.* **1999**, *40*, 1519. (b) Kotani, M.; Yamago, S.; Satoh, A.; Tokuyama, H.; Fukuyama, T. *Synlett* **2005**, *12*, 1893. (c) Fukuyama, T.; Chen, X.; Peng, G. *J. Am. Chem. Soc.* **1994**, *116*, 3127. (d) Tokuyama, H.; Fukuyama, T. *Chem Record* **2002**, *2*, 37.

⁴⁹ (a) Evoniuk, C. J.; Ly, M.; Alabugin, I. V. *Chem. Commun.* **2015**, *51*, 12831. (b) Evoniuk, C. J.; Gomes, G. P.; Ly, M.; White, F. D. and Alabugin, I. V. *J. Org. Chem.*, **2017**, *82*, 4265. (c) Gomes, G. P.; Evoniuk, C.; Ly, M.; Alabugin, I. V. *Org. Biomol. Chem.*, **2017**, *15*, 4135.

⁵⁰ For an insightful explanation to why bonds next to a nitrogen are weakened, see Borden, W. T. *J. Phys. Chem. A.*, **2017**, *121*, 1140.

TOC Graphics:

isonitriles are
stereochemical *chameleons*

